Original Article

Weighted miRNA co-expression network reveals potential roles of apoptosis related pathways and crucial genes in thoracic aortic aneurysm

Siliang Chen[1#], Lei Ji[1#], Mengyin Chen[1], Dan Yang[2], Jiawei Zhou[1], Yuehong Zheng[1]

[1]Department of Vascular Surgery, Peking Union Medical College Hospital, Chinese Academy of Medical Sciences and Peking Union Medical College, Beijing, China; [2]Department of Computational Biology and Bioinformatics, Institute of Medicinal Plant Development, Chinese Academy of Medical Sciences and Peking Union Medical College, Beijing, China

Contributions: (I) Conception and design: S Chen, D Yang, Y Zheng; (II) Administrative support: D Yang, Y Zheng; (III) Provision of study materials or patients: S Chen, D Yang; (IV) Collection and assembly of data: S Chen, L Ji, M Chen, J Zhou; (V) Data analysis and interpretation: S Chen, L Ji, M Chen, D Yang; (VI) Manuscript writing: All authors; (VII) Final approval of manuscript: All authors.

[#]These authors contributed equally to this work.

Correspondence to: Yuehong Zheng. No. 1 Shuai Fu Yuan, Dongcheng District, Beijing 100730, China. Email: yuehongzheng@yahoo.com.

Background: Thoracic aortic aneurysm (TAA) is a potentially life-threatening disease for which few medical therapies are available. Thus, it is critically important to investigate the underlying molecular mechanisms of TAA, and identify potential targets for TAA treatment.

Methods: Differentially expressed miRNAs (DEMs) and differentially expressed genes (DEGs) were screened, and a weighted correlation network analysis (WGCNA) was employed to construct a weighted miRNA co-expression network using GSE110527. The DEMs were then mapped into the whole co-expression network of all samples, and a DEM coexpression network was created. Molecular Complex Detection (MCODE) was used to identify crucial miRNAs. Target genes were predicted using the miRTarbase database, and further screened by identifying genes that overlapped with the DEGs of GSE26155. The screened target genes were validated using GSE9106, and the successfully validated genes were considered as crucial genes. Finally, a miRNA risk score for diagnosing TAA was calculated by undertaking a least absolute shrinkage and selection operator (LASSO) regression.

Results: The tumor necrosis factor (TNF)-related apoptosis-inducing ligand (TRAIL) signaling pathway was found in DEM functional enrichment. Crucial miRNAs were identified and target genes were predicted and associated with the regulation of the TRAIL signaling pathway. Next, 113 important target genes were identified as overlapping with the DEGs of GSE26155. These genes were further validated, and 5 successfully validated genes were considered as crucial genes. Finally, the miRNA risk score calculated by the LASSO regression was shown to have potential diagnostic value.

Conclusions: We performed a WGCNA analysis to construct a weighted miRNA co-expression network, predicted target genes of crucial miRNAs, identified crucial genes, and finally calculated a miRNA risk score. The results showed that pathways and genes associated with apoptosis appear to play an important role in TAA pathogenesis, and that medications targeting apoptosis might slow TAA progression. Future *in vitro* and *in vivo* experimental studies need to be undertaken to further validate our findings and investigate the mechanistic details of these crucial miRNAs and crucial genes.

Keywords: Thoracic aortic aneurysm (TAA); miRNA; weighted correlation network analysis (WGCNA); apoptosis

Submitted Dec 28, 2020. Accepted for publication Mar 14, 2021.

doi: 10.21037/jtd-20-3601

View this article at: http://dx.doi.org/10.21037/jtd-20-3601

Introduction

Thoracic aortic aneurysm (TAA) is a potentially life-threatening disease with an incidence of approximately 10 in 100,000 persons per year (1). Most patients with TAA are asymptomatic, and the major risk associated with TAA is aneurysm rupture, which is associated with high mortality (2). To date, surgical interventions, especially endovascular repairs, are the first-line procedure for treating TAA. However, such surgical procedures are often complicated (3). Thus, it is critically important to investigate the underlying molecular mechanisms of TAA and to identify potential targets for TAA treatment. The pathogenesis of TAA is complex and includes the apoptosis of vascular smooth muscle cells (VSMCs), chronic inflammation, and oxidative stress (4-6). Over the past decade, a number of studies have demonstrated that genetic factors play an important role in the initiation and progression of TAA (7-9). Based on a genome-wide analysis, the genes associated with pathologies of TAA, such as those associated with VSMC contractility, have been discovered (10).

Through transcriptome, miRNAs have been explored in TAA patients or mouse models. In a recent study, a miRNA microarray assay identified 232 differentially expressed miRNAs (DEMs), and miR-574-5p was confirmed and validated as a possible therapeutic target in serum, mouse, and cellular experiments (11). Another study using tissue and plasma samples with NanoString nCounter technology also revealed 3 miRNAs that might serve as biomarkers for ascending TAA patients (12). However, it is insufficient to focus on the differential expression status of miRNAs between TAA and control groups, as the potential interactions between the miRNAs and the crucial miRNAs that might mediate TAA pathogenesis also need to be explored. To address this, several methods have been developed to focus on genes with similar expression patterns that may participate in a specific pathogenesis. Of these methods, the most widely used is the weighted correlation network analysis (WGCNA) (13). WGCNA can be used to construct a weighted co-expression network for genes, detect gene modules, associate gene modules with clinical traits, and mine crucial genes that could potentially mediate important biological processes. Furthermore, WGCNA can also be applied to construct co-expression networks based on noncoding RNA, such as miRNA (14,15). The WGCNA has been used to construct gene co-expression networks and identify crucial genes mediating abdominal aortic aneurysm (AAA) based on mRNA expression data (16). In TAA, a miRNA-target derived from the Kyoto Encyclopedia of Genes and Genomes (KEGG) pathway network examined the role of Krüppel-like factor 4 in the pathogenesis of TAA (17). In a recently published study, WGCNA was conducted on mRNA expression data of AAA, TAA, and intracranial aneurysm. The results of this study identified conserved gene modules between different types of aneurysms. This study then mined hub genes, built miRNA-hub gene network using miRNet, and identified several crucial genes and miRNAs based on this network (18). However, to date, very few studies have directly constructed a weighted miRNA co-expression network by undertaking WGCNA in TAA.

In the present study, we constructed a co-expression work based on a miRNA data set of TAA (GSE110527). The DEMs were mapped into the whole miRNA co-expression network of TAA, and a DEM co-expression network was constructed. Crucial miRNAs were mined based on the DEM co-expression network. Target genes were predicted for crucial miRNAs, and were compared with differentially expressed genes (DEGs) of an mRNA data set of TAA (GSE26155). Overlapping target genes were identified as important target genes. Another independent mRNA data set (GSE9106) was used to validate these genes; the successfully validated genes were considered as crucial genes. Finally, a miRNA risk score was also calculated by performing least absolute shrinkage and selection operator (LASSO) regression to show the potential clinical significance of miRNA in a DEM co-expression network.

We present the following article in accordance with the MDAR checklist (available at http://dx.doi.org/10.21037/jtd-20-3601).

Methods

Medical ethics

The study was conducted in accordance with the Declaration of Helsinki (as revised in 2013). The raw data sets were obtained from the Gene Expression Omnibus (GEO) database (http://www.ncbi.nlm.nih.gov/geo/; GSE110527, GSE26155, and GSE9106). In this study, no human trials or animal experiments were conducted.

Data sets and data preprocessing

Three GEO data sets (GSE110527, GSE26155, and GSE9106) were included in our study. GSE110527 is

a miRNA microarray data set containing 19 TAA and 19 normal thoracic aorta samples, and was used in the construction of miRNA co-expression network. GSE26155 and GSE9106 are 2 mRNA microarray data sets containing aortic samples and plasma samples, respectively. These 2 data sets were used for crucial mRNA mining. The series matrix files were downloaded from the GEO database, and all the data sets were converted into $\log_2$-transformed format before being subjected to further analysis. For the mRNA microarray data sets, the microarray platform data tables were also downloaded to annotate probe IDs in the series matrix files with a gene symbol.

DEM and DEG screening

The "limma" R package was used to conduct a DEM analysis for GSE110527, and a DEG analysis for GSE26155 and GSE9106. For the DEM analysis, a threshold of $|\log_2(\text{fold-change})|>1$ and an adjusted P value of <0.01 were chosen. For the DEG analysis, a threshold of adjusted P<0.05 was chosen. To explore the biological processes and pathways in which these DEMs were involved, the DEMs were subjected to FunRich v3.1.3 for a functional enrichment analysis. For the DEGs, the "clusterProfiler" R package was used to conduct a functional enrichment analysis.

miRNA co-expression network construction

The "WGCNA" R package was used to create a miRNA co-expression network for the TAA samples. The miRNAs with the highest 25% variance were included in further analysis. A Pearson's correlation matrix was calculated and transformed into an adjacency matrix using the following formula: $a_{mn} = |c_{mn}|^{\beta}$ (where a_{mn} represents adjacency between miRNA m and miRNA n, c_{mn} represents Pearson's correlation coefficient between miRNA m and miRNA n, and β represents the soft threshold). The adjacency matrix stored the information of the whole network. To identify miRNA modules, a topological overlap matrix (TOM) was built based on the adjacency matrix, and a dynamic tree-cut algorithm was used to allocate miRNAs to different modules. The minimal module size was set at 100, and a threshold of 0.25 was selected to merge similar miRNA modules. FunRich was also used to conduct a functional enrichment analysis of the miRNAs of each module.

DEM co-expression network construction and crucial miRNA mining

We mapped DEMs into the whole co-expression network of all samples in Cytoscape v3.7.0 and created a DEM co-expression network. Molecular Complex Detection (MCODE), a plugin in Cytoscape that detects densely connected regions in a network, was applied to the DEM co-expression network. The most significant MCODE cluster was chosen. We considered miRNAs with top-10 degree in this cluster as crucial miRNAs.

Target prediction and crucial mRNA mining

To obtain an appropriate number of target genes for further mining and to minimize the false-positive rate, the miRTarbase database (http://mirtarbase.cuhk.edu.cn/php/index.php), a literature-based miRNA-target interactions prediction tool, was employed to predict the target genes of crucial miRNAs. The biological processes and pathways for these genes were also shown using a "clusterProfiler" package. After the prediction of the target genes, the overlap between these target genes and DEGs in GSE26155 were used to obtain the important target genes. Finally, another independent database was used to validate these important target genes; the successfully validated target genes were considered as crucial genes.

LASSO regression and the calculation of a miRNA risk score

The stability of the miRNAs raises the possibility of their being used as disease biomarkers (19). To further evaluate the potential diagnostic value of miRNAs, we adopted a machine-learning approach whereby we undertook a LASSO regression to calculate a miRNA risk score. Important variables with nonzero coefficients that can accurately predict disease status can be screened by a LASSO regression. The "glmnet()" function in the "glmnet" R package was used to conduct a LASSO regression to select which miRNAs would be the most useful in the prediction of TAA. To ensure the robustness of the selected variables, a 10-fold cross-validation was performed using the "cv.glmnet()" function. Based on the minimal 1-standard error (SE) criterion, the optimal λ was chosen to obtain the coefficients for the variables. A miRNA risk score was calculated through a linear combination of selected variables

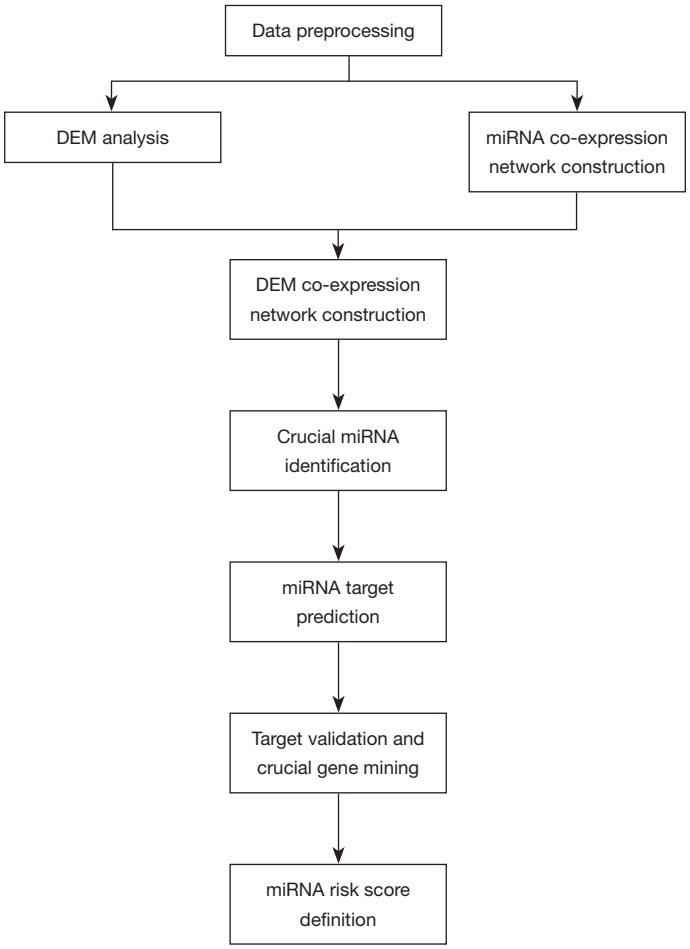

Figure 1 Flowchart of the whole study. DEM, differentially expressed miRNA.

that were weighted by their corresponding coefficients. A receiver operating characteristics (ROC) analysis was undertaken to determine the diagnostic value of this miRNA risk score.

Statistical analysis

Data preprocessing, the DEM and DEG analyses, the WGCNA analysis, the functional enrichment analysis of the DEGs and the target genes, the LASSO regression and a cross-validation were conducted in R v.3.6.2 (The R Foundation for Statistical Computing). The details of these bioinformatic analyses are described in corresponding subsections, and codes for these analyses are available in the Supplementary Data. The ROC analysis was conducted using SPSS 25.0 (IBM Corp). A P value of <0.05 was considered significant.

Results

Flowchart of the whole study

Figure 1 shows a flowchart of our study. After data downloading and preprocessing, we conducted DEM, DEG, and WGCNA analyses. We mapped DEMs into the whole miRNA co-expression network of TAA and created a DEM co-expression network. MCODE was then used to detect the most significant cluster, and miRNAs with the top-10 degree were considered as crucial miRNAs. The miRTarbase database was used to find literature-based target genes of crucial miRNAs. Any genes that overlapped between the target genes and DEGs of GSE26155 were identified as important target genes. Another independent data set (GSE9106) was employed to validate these important target genes, and the successfully validated genes were considered as crucial genes. Finally, a LASSO

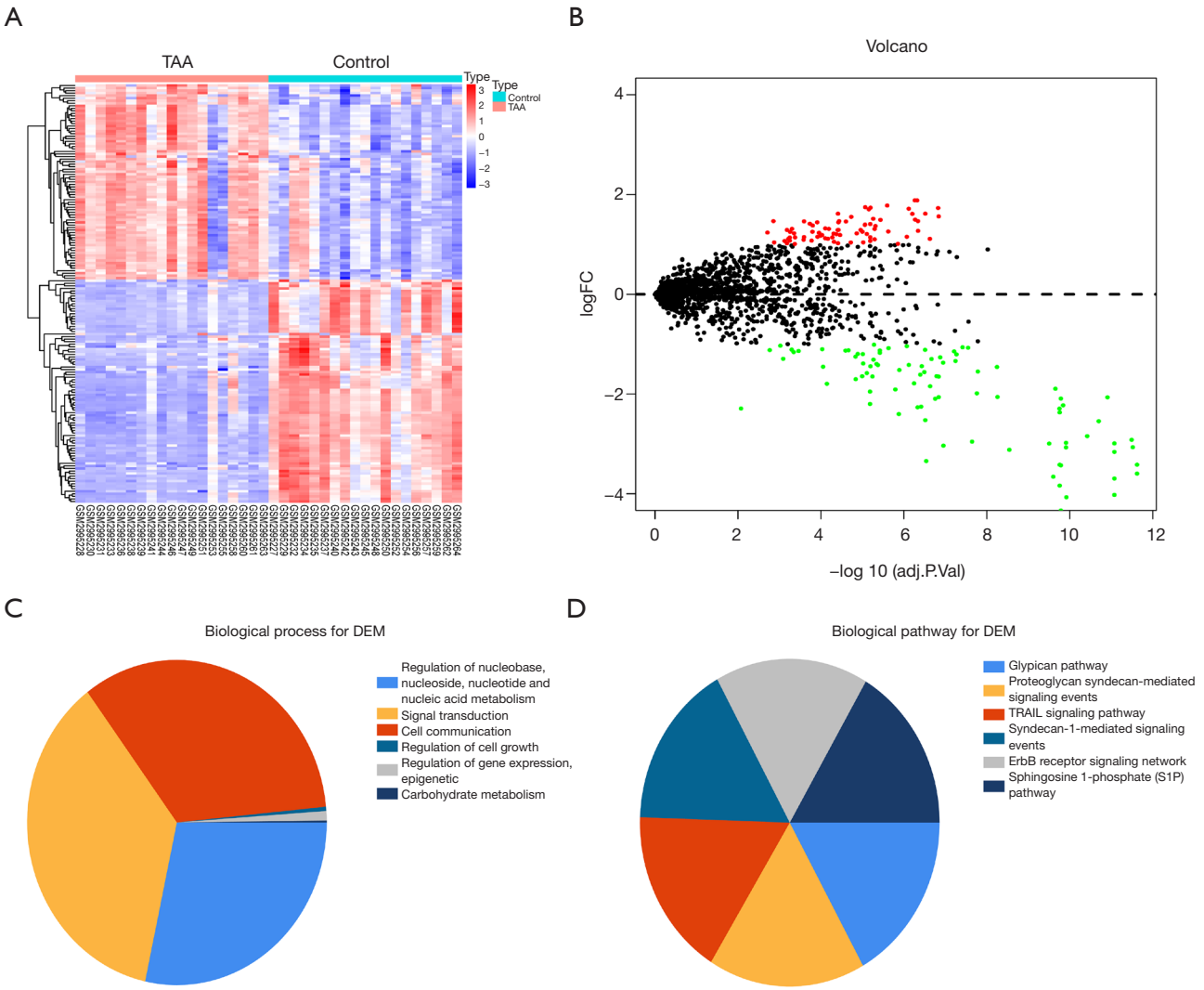

Figure 2 Screening of DEMs. (A) Heatmap for DEMs. The red color represents upregulation, and the blue color represents downregulation. (B) Volcano plot for DEMs. The red dots represent up-regulated genes while the green dots represent down-regulated genes. (C) Biological processes for DEMs with top-6 significance. (D) Biological pathways for DEMs with top-6 significance. DEM, differentially expressed miRNA; TAA, thoracic aortic aneurysm.

regression was used to calculate a miRNA risk score to show the potential diagnostic value of miRNAs in the most significant MCODE cluster.

Screening of DEMs and DEGs

Using the threshold of $|\log_2(\text{fold-change})|>1$ and adjusted P value of <0.01, a total of 165 DEMs were screened. Of these, 77 were up-regulated and 88 were down-regulated (*Figure 2A,B*). *Table 1* shows DEMs with top-10 $|\log_2(\text{fold-change})|$ and the most significant genes and pathways interacting with DEMs. *Figure 2C,D* and Table S1 show the biological processes and pathways of all DEMs. For GSE26155 and GSE9160, a total of 1,965 and 2,368 DEGs were screened, respectively (*Figure 3* and https://cdn.amegroups.cn/static/public/jtd-20-3601-1.xlsx). Figure S1 and https://cdn.amegroups.cn/static/public/jtd-20-3601-2.xlsx show the results of the functional enrichment analysis

Table 1 DEMs with top-10 |$\log_2$(fold-change)|. The most significant gene and pathway related to these DEMs were also listed. These genes were derived from combination of DEGs and target genes and these pathways were derived from KEGG pathway analysis

miRNA	$\log_2$(fold-change)	Adjusted P	Associated gene and pathway
Up-regulated			
hsa-miR-377-3p	1.88326	5.44E-07	CD93/prostate cancer
hsa-miR-337-5p	1.882185	4.80E-07	HOXB7/regulation of transcription, DNA-templated
hsa-miR-376a-3p	1.779841	2.52E-06	KIF5C/prostate cancer
hsa-miR-128-3p	1.746482	8.53E-06	NR2F2/signaling pathways regulating pluripotency of stem cells
hsa-miR-127-3p	1.737214	6.36E-06	MAPK4/regulation of apoptotic process
hsa-miR-495-3p	1.730242	1.50E-07	MARCKS/herpes simplex infection
hsa-miR-136-3p	1.715058	7.64E-07	ASAP1/cell projection organization
hsa-miR-376c-3p	1.704712	7.00E-06	DAPK1/proteoglycans in cancer
hsa-miR-379-5p	1.615944	3.05E-07	LNPEP/hematopoietic cell lineage
hsa-miR-487b-3p	1.615856	3.87E-05	SOBP/signaling pathways regulating pluripotency of stem cells
Down-regulated			
hsa-miR-670-5p	–3.41621	2.39E-12	GRAP2/axon guidance
hsa-miR-4726-5p	–3.41707	1.75E-10	HOXA3/oxidative phosphorylation
hsa-miR-6847-5p	–3.42813	1.64E-10	COL1A1/p53 signaling pathway
hsa-miR-3148	–3.59477	2.39E-12	GPR75/oocyte meiosis
hsa-miR-205-3p	–3.65704	2.51E-10	CLEC2D/pathways in cancer
hsa-miR-32-3p	–3.69307	8.43E-12	ZNF587/hippo signaling pathway
hsa-miR-6130	–3.83502	1.75E-10	FMNL3/viral carcinogenesis
hsa-miR-3149	–4.02192	8.43E-12	MBOAT2/transcription, DNA-templated
hsa-miR-6817-5p	–4.0683	1.21E-10	ZNF85/3'-UTR-mediated mRNA stabilization
hsa-miR-6805-5p	–4.33394	1.64E-10	NDRG1/carbon metabolism

DEM, differentially expressed miRNA; DEG, differentially expressed gene; KEGG, Kyoto Encyclopedia of Genes and Genomes.

for the DEGs. Pathways related to apoptosis, such as the tumor necrosis factor (TNF)-related apoptosis-inducing ligand (TRAIL) signaling pathway, appeared in the top-6 significant pathways.

Construction of miRNA co-expression network

No outliers were excluded and all samples were involved in the network construction (Figure S2A). Using a cutoff of R^2=0.9, a soft threshold of β=5 was chosen (Figure S2B,S2C). As the histogram and linear plot show, the network that we constructed met the requirement of a scale-free topology with an R^2 of 0.91 (Figure S2D,S2E). The miRNA expression modules were then detected based on the TOM, and a total of 4 modules were obtained (Figure S2F). A functional enrichment analysis was conducted for the miRNAs in each module (Figure S3).

Mining of crucial miRNAs

DEMs were mapped into the whole co-expression network of all samples, and a DEM co-expression network was created (Figure S4). MCODE was employed to identify densely connected network regions, and the most significant MCODE cluster with 159 nodes and 12,388 edges was included in further analysis (*Figure 4A*). miRNAs with the top-10 degree in the MCODE cluster were considered as crucial miRNAs (*Figure 4B*).

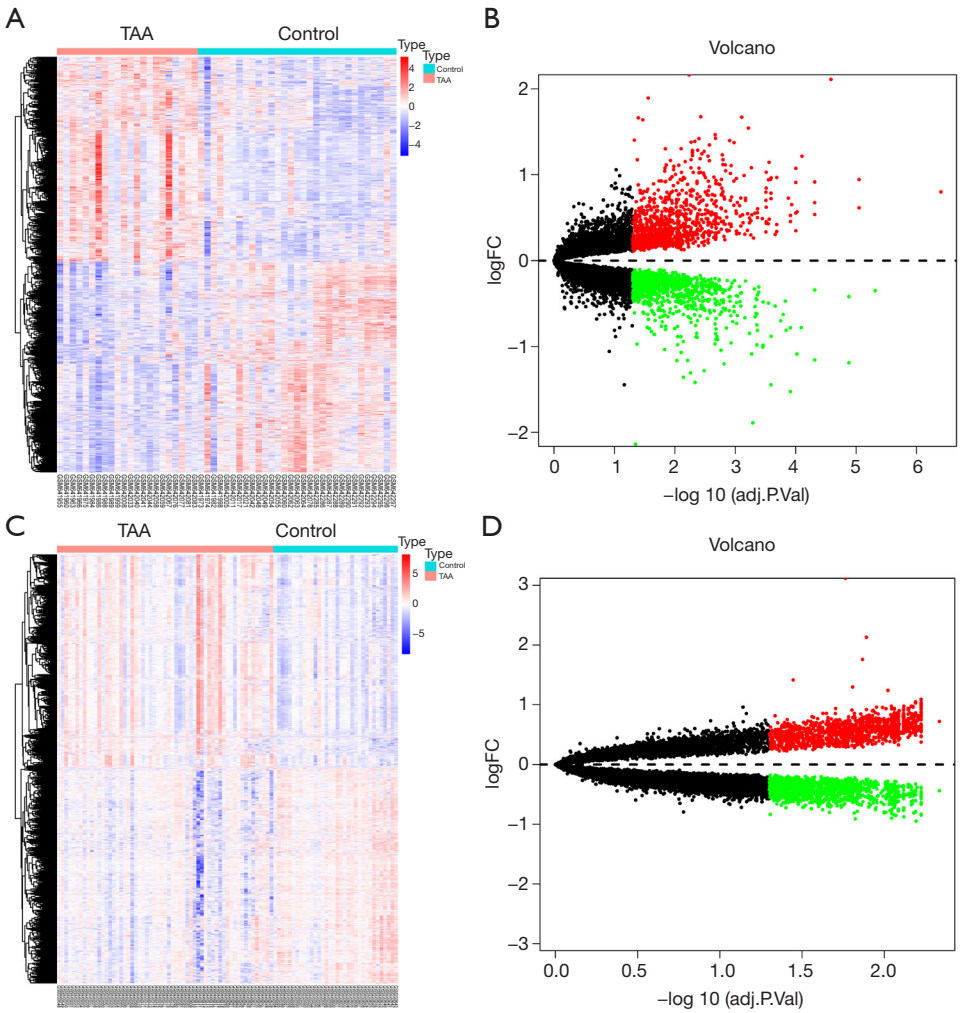

Figure 3 Screening of DEGs. (A,B) Heatmap and volcano plot showing the expression patterns of GSE26155. (C,D) Heatmap and volcano plot showing the expression patterns of GSE9106. DEG, differentially expressed gene; TAA, thoracic aortic aneurysm.

Target prediction and mining of crucial genes

The target genes of crucial miRNAs were predicted using the miRTarbase database (https://cdn.amegroups.cn/static/public/jtd-20-3601-3.xlsx), and a total of 994 target genes were predicted. *Figure 5* and Table S2 show the Gene Ontology (GO) and KEGG pathway enrichment analyses of these genes. The regulation of the apoptotic signaling pathway (ASP) was the GO term with the highest count number. These genes were then compared with the DEGs of GSE26155, and 113 overlapping genes were identified (*Figure 6A*). These overlapping genes were validated using the DEGs of GSE9160, and 5 crucial genes were identified (*Figure 6B* and *Table 2*).

Calculating a miRNA risk score to predict TAA

A total of 11 miRNAs with a nonzero coefficient were screened by the LASSO regression (Figure S5A,S5B). *Table 3* shows the areas under the curves (AUCs) of these 11 miRNAs. Notably, most of these miRNAs (8 of 11) had AUCs higher than 0.9. The risk score was calculated through a linear combination of the 11 miRNAs weighted by their coefficients (Table S3). An ROC analysis showed the potential diagnostic value of the miRNA risk score with an AUC of 1 (SE =6.73E-9, P=1.37E-7; Figure S5C).

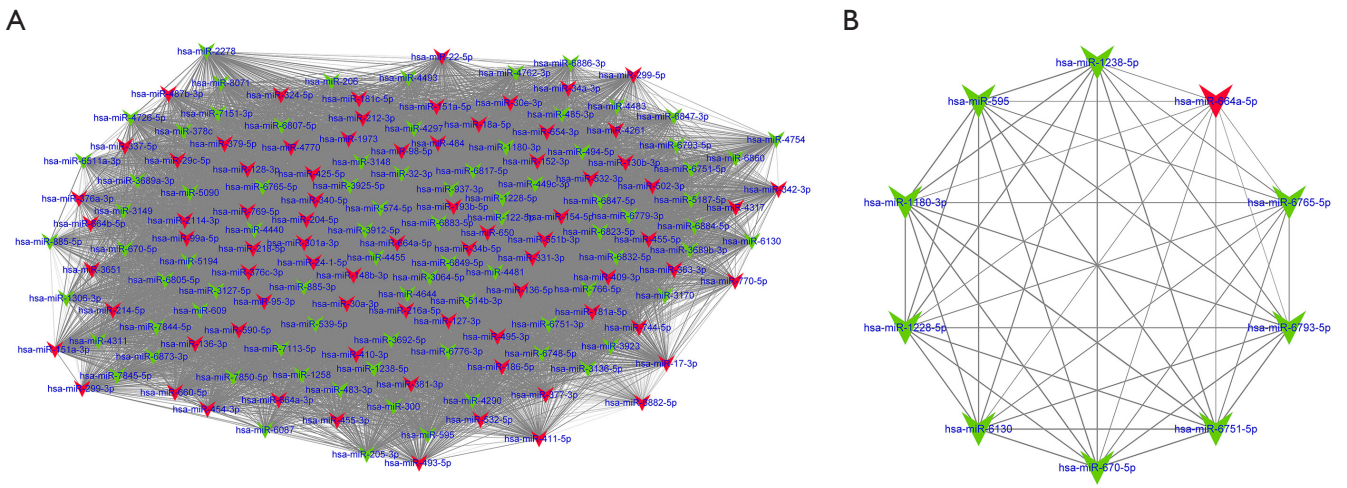

Figure 4 Crucial miRNA identification. (A) The most significant MCODE cluster based on the DEM co-expression network. (B) Crucial miRNAs with the top-10 degree. DEM, differentially expressed miRNA; MCODE, Molecular Complex Detection.

Summary of main findings

In the present study, a DEM analysis was first conducted, and a total of 165 DEMs were screened. A miRNA co-expression network of TAA was then constructed and combined with DEMs to obtain a DEM co-expression network. MCODE was applied to detect densely connected regions in the DEM co-expression network, and miRNAs with the top-10 degree in the most significant MCODE cluster were selected as crucial miRNAs. A total of 994 target genes for crucial miRNAs were predicted, and 113 overlapping genes were identified after comparing target genes with the DEGs of GSE26155. Next, these genes were validated using another independent data set (GSE9106), and 5 crucial genes were identified. Finally, a miRNA risk score was constructed by a LASSO regression based on miRNAs in the MCODE cluster.

Discussion

The functional enrichment analysis showed that DEMs participate in multiple biological processes. The TRAIL signaling pathway was among the top-6 significant biological pathways for DEMs. The TRAIL signaling pathway is thought to be vital in the induction of cell apoptosis (20). Gonçalves *et al.* (21) showed that TRAIL activation induced the apoptosis of VSMCs *in vitro*. Consistent with previous studies, the findings of the present study suggest that TRAIL-induced apoptosis might play a role in TAA pathogenesis (22). Apoptosis-related pathways were also found in the functional enrichment analysis of target genes. The regulation of ASP is an enriched pathway with the highest count number. ASP can be divided into two categories: intrinsic and extrinsic ASP. Several pathways associated with intrinsic ASP were also found in the functional enrichment analysis of target genes. Intrinsic ASP could be induced by DNA damage, and p53 is the central effector molecule in DNA damage response (23). Previous research has shown that DNA damage-induced agents, such as chemotherapeutic drugs and irradiation, could cause apoptotic death through a p53-dependent pathway (24). Zhang *et al.* found that p53-dependent VSMC senescence plays a role in the development of TAA (25), and several studies have documented p53-dependent VSMC apoptosis in AAA (26,27). The second category of ASP is extrinsic ASP. The TRAIL pathway, which was shown in the biological pathway analysis of DEMs in our study, can initiate the extrinsic ASP through the formation of the death-inducing signaling complex, followed by the activation of effector caspases (28,29). The above-mentioned results emphasize the importance of gaining a comprehensive understanding of apoptosis in TAA pathogenesis.

By further screening important target genes and using an independent data set to validate these genes, 5 crucial genes were identified. Of these genes, the expression of B-cell lymphoma 2 like 1 (BCL2L1), retinoic acid receptor alpha (RARα), and nuclear receptor interacting protein 2 (NRIP2) were higher in the TAA group, and the expressions of

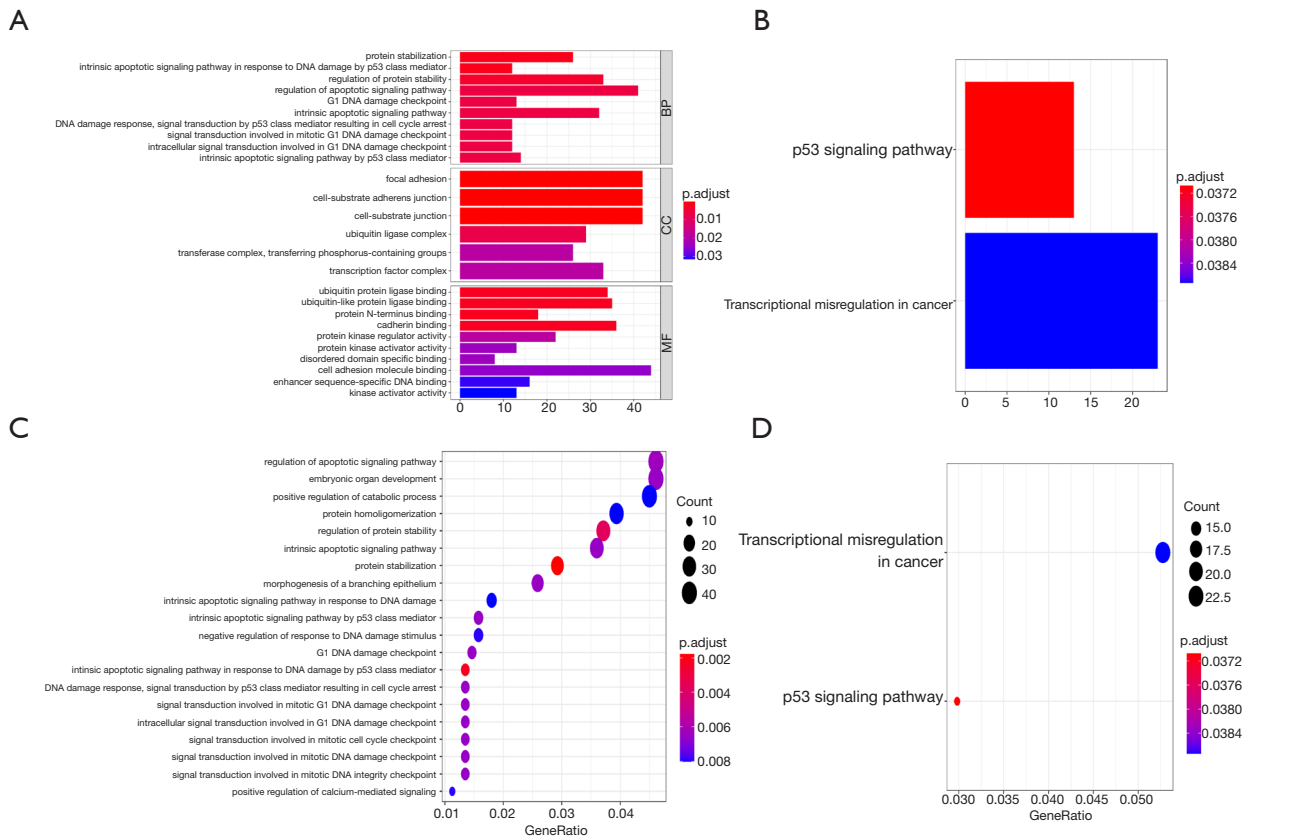

Figure 5 Functional enrichment analysis of target genes for crucial miRNAs predicted by the miRTarbase database. (A,B) Bar plot for GO (BP, biological process; CC, cellular component; MF, molecular function) and KEGG pathway analysis. Terms with top-10 significant adjusted P value were shown and ordered according to adjusted P value. (C,D) Dot plot for GO and KEGG pathway analysis. Terms with top-20 count number were ordered according to count number. For all these plots, redder color indicates smaller adjusted P value while bluer color indicates larger adjusted P value and all the adjusted P values of these terms were <0.05. Apoptosis related pathways were found in the functional enrichment analysis. GO, Gene Ontology; KEGG, Kyoto Encyclopedia of Genes and Genomes.

the other 2 genes were lower with limited studies. The protein encoded by BCL2L1 belongs to the BCL2 protein family. Genes with varying degrees of homology to BCL2 have been identified that code for both antiapoptotic and proapoptotic proteins. As a result of alternative splicing, BCL2L1 has two isoforms (i.e., Bcl-xl and Bcl-xs). These two isoforms have opposite effects in regulating apoptosis. Bcl-xl is the longer isoform with antiapoptotic activity, while Bcl-xs is the shorter isoform with proapoptotic activity (30). The overexpression of Bcl-xs causes the mitochondrial activation of a caspase cascade through the release of cytochrome c, and antagonizes the antiapoptotic effects of Bcl-xl (31,32). Bcl-xs might play an important role in vascular diseases. Okura *et al.* found that platelet-derived growth factor (PDGF)-BB induced apoptosis of VSMCs *in vitro*, and caused a decrease in Bcl-xl and an increase in Bcl-xs (33). In an *in vivo* experiment, Bcl-xs was found to be up-regulated in balloon-injured carotid arteries in a rat model. These findings suggest that Bcl-xs might be a crucial mediator of VSMC apoptosis. Although Durdu *et al.* found that BCL2L1 was down-regulated in TAA compared with control group in immunohistochemical staining with a borderline P value (P=0.49) (31,32,34), the role of Bcl-xs in apoptosis still provided us with a new perspective to understand TAA pathogenesis.

RARα is a nuclear RAR that has been implicated in crucial biological processes, such as development, differentiation, and apoptosis (35). Fusion protein PML/RARα inhibits the differentiation and apoptosis of myeloid precursor cells, causing acute promyelocytic leukemia (APL) (36).

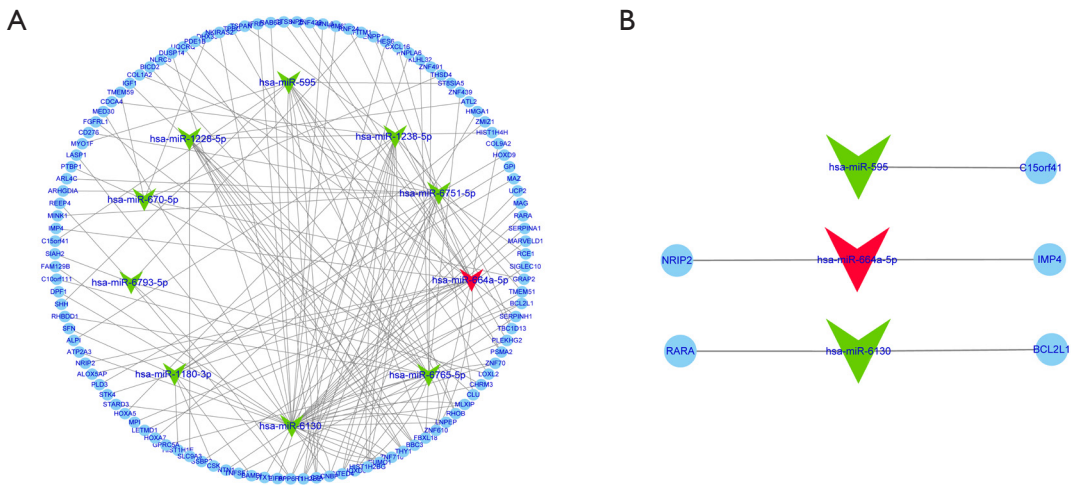

Figure 6 Crucial gene identification. (A) Interactions between crucial miRNAs and important target genes derived from overlaps between target genes for crucial miRNAs and DEGs for GSE26155. (B) Interactions between crucial miRNAs and validated crucial genes. DEG, differentially expressed gene.

Retinoids represent a promising treatment for APL. Indeed, Altucci *et al.* revealed that the all-trans retinoic acid, one of the RARα agonist, induced apoptosis in NB4 cells. Additionally, the activation of RARα has also been shown to induce the expression of TRAIL and thus cause apoptosis (37). Our findings that RARα was up-regulated in the TAA group and TRAIL signaling pathways in the DEM functional enrichment analysis suggest that RARα-induced apoptosis might also play a role in TAA pathogenesis.

NRIP2 belongs to the aspartic protease family, and can bind directly to the C-terminal ligand binding domain of mouse retinoic acid receptor β (RORβ) to inhibit the transcriptional activity of RORβ (38,39). Wen *et al.* found that NRIP2 could up-regulate the Wnt signaling pathway in colorectal cancer by targeting RORβ (40). Activated Wnt signaling pathway was observed in both TAA and AAA (37,41,42). It is not clear whether the Wnt pathway participates in TAA pathogenesis through apoptosis; however, studies have shown that the Wnt signaling pathway might be involved in aneurysm pathogenesis by inducing inflammation, up-regulating MMPs, and promoting endothelial cell senescence. It could be inferred that NRIP2 might participate in TAA pathogenesis by up-regulating the Wnt signaling pathway and possibly participate apoptosis.

The pathway analyses and the identification of the crucial genes showed that apoptosis might play an important role in TAA pathogenesis, with VSMCs also being implicated in this disease. VSMCs and elastic fibers are the main components of tunica media, and maintain the tensile strength and elasticity of the aorta (43). Additionally, as Shanahan summarized, VSMCs also serve as central mediators in vascular wall inflammation through crosstalk with endothelial cells and immune cells. VSMC apoptosis not only contributes to the destabilization of the vascular wall, but also enhances inflammation and oxidative stress and shifts the vascular microenvironment toward a proteolytic state. The roles of miRNA in VSMCs have been subjected to more investigation in the murine aneurysmal model. Notably, Woo *et al.* explored how the interactions between 30b-5p miRNA and MBNL1 mRNA participate in human coronary atherosclerosis by mediating VSMC differentiation (44) and similar studies should seek to test the role of VSMCs in human TAA.

Finally, we made a miRNA risk score system for TAA for which we obtained a quite good AUC value. Over the past decade, miRNAs have been accepted as potential diagnostic markers or prognostic biomarkers for diseases of different organs. For example, a recent study developed a novel prognostic signature that excellently predicted the 1- and 3-year survival rate of patients with glioma (45). Another study on pancreatic cancer established a risk score system using 7 miRNAs to predict overall survival and recurrence-free survival, which showed reliable performance with a high C-index (46). To the best of our knowledge, this study is the first to report a miRNA risk score system in TAA.

In the present study, we constructed a miRNA co-expression network in TAA for the first time, and identified

Table 2 Validated crucial genes

Gene symbol	Official full name	log_2(fold-change)	Adjusted P
BCL2L1	BCL2 like	0.283648	0.007205
C15orf41	Chromosome 15 open reading frame 41	−0.24887	0.044316
IMP4	IMP U3 small nucleolar ribonucleoprotein 4	−0.19898	0.032765
NRIP2	Nuclear receptor interacting protein 2	0.203744	0.032021
RARA	Retinoic acid receptor alpha	0.293798	0.011716

Table 3 AUCs for lasso selected miRNAs

miRNAs	AUC	SE	P value
hsa-miR-6882-5p	0.911	0.045	<0.001
hsa-miR-885-5p	0.934	0.042	<0.001
hsa-miR-7845-5p	0.983	0.018	<0.001
hsa-miR-7844-5p	0.992	0.010	<0.001
hsa-miR-6849-5p	0.970	0.023	<0.001
hsa-miR-6847-5p	0.972	0.023	<0.001
hsa-miR-206	0.992	0.010	<0.001
hsa-miR-6807-5p	0.975	0.021	<0.001
hsa-miR-1306-3p	0.945	0.038	<0.001
hsa-miR-128-3p	0.898	0.050	<0.001
hsa-miR-551b-3p	0.834	0.073	<0.001

AUC, area under curve; SE, standard error.

crucial miRNAs based on a DEM co-expression network. The target genes of these crucial miRNAs were predicted using a literature-based miRNA-target interaction prediction tool (i.e., the miRTarbase database). Important target genes were identified as the overlapping genes of the target genes and DEGs in a TAA mRNA microarray data set. Then we validated these important target genes using another independent data set; the successfully validated genes were considered as crucial genes.

However, it should be noted that this study had a number of limitations. First, the 3 data sets used had some discrepancies in TAA localization and clinical causes. Detailed grouping information about these discrepancies was not provided, and we cannot conduct a subgroup analysis to examine the effect of the heterogeneity. Second, we made a compromise to choose GSE9106, which was based on plasma samples, as our validation set, as there were no other available or appropriate data sets using aortic tissue that could be used for validation (47). Third, to simultaneously obtain an appropriate number of target genes for further mining and minimize the false-positive rate, we only used one a single target gene prediction tool, although it's literature-based. In addition, due to the lack of detailed clinical information in the GEO database we could not associate miRNA modules with clinical traits. Finally, while our study found that apoptosis might potentially play an important role in TAA pathogenesis based on miRNA co-expression network, other epigenetic mechanisms, such as epigenetic modulations in VSMCs by histone deacetylases, are also potential contributors to TAA pathogenesis and require further exploration (48).

Conclusions

We performed a WGCNA analysis to construct a weighted miRNA co-expression network, predicted target genes

of crucial miRNAs, identified crucial genes, and finally calculated a miRNA risk score. Heterogeneity regarding TAA localization and clinical causes exists; however, our study still has implications for translational application, as TAAs share common pathophysiological features, such as the loss of VSMCs, extracellular matrix degradation, and proteoglycan deposition (43,49,50). Our study revealed that pathways and genes associated with apoptosis might play an important role in TAA pathogenesis, and medications targeting apoptosis might be promising therapies to slow TAA progression. Future *in vitro* and *in vivo* experimental studies need to be conducted to further validate our findings and investigate the mechanistic details of these crucial miRNAs and genes.

Acknowledgments

We thank English Language Editors L. Huleatt and J. Gray for their polishing of our manuscript.
Funding: This work was supported by the Natural Science Foundation of China (No. 81770481 and No. 51890894) and CIFMS 2017-I2M-1-008)/Chinese Academy of Medical Sciences, innovation Fund for Medical Sciences (CIFMS 2017-I2M-1-008). The funders had no role in the design of the study, data collection and analysis, decision to publish, or preparation of the manuscript.

Footnote

Reporting Checklist: The authors have completed the MDAR checklist. Available at http://dx.doi.org/10.21037/jtd-20-3601

Peer Review File: Available at http://dx.doi.org/10.21037/jtd-20-3601

Conflicts of Interest: All authors have completed the ICMJE uniform disclosure form (available at http://dx.doi.org/10.21037/jtd-20-3601). The authors have no conflicts of interests to declare.

Ethical Statement: The authors are accountable for all aspects of the work in ensuring that questions related to the accuracy or integrity of any part of the work are appropriately investigated and resolved. The study was conducted in accordance with the Declaration of Helsinki (as revised in 2013).

References

1. Elefteriades JA, Sang A, Kuzmik G, et al. Guilt by association: paradigm for detecting a silent killer (thoracic aortic aneurysm). Open Heart 2015;2:e000169.
2. Erbel R, Aboyans V, Boileau C, et al. 2014 ESC Guidelines on the diagnosis and treatment of aortic diseases: Document covering acute and chronic aortic diseases of the thoracic and abdominal aorta of the adult. The Task Force for the Diagnosis and Treatment of Aortic Diseases of the European Society of Cardiology (ESC). Eur Heart J 2014;35:2873-926.
3. Elefteriades JA, Farkas EA. Thoracic aortic aneurysm clinically pertinent controversies and uncertainties. J Am Coll Cardiol 2010;55:841-57.
4. Nataatmadja M, West M, West J, et al. Abnormal extracellular matrix protein transport associated with increased apoptosis of vascular smooth muscle cells in marfan syndrome and bicuspid aortic valve thoracic aortic aneurysm. Circulation 2003;108 Suppl 1:II329-34.
5. He R, Guo DC, Sun W, et al. Characterization of the inflammatory cells in ascending thoracic aortic aneurysms in patients with Marfan syndrome, familial thoracic aortic aneurysms, and sporadic aneurysms. J Thorac Cardiovasc Surg 2008;136:922-9, 929.e1.
6. Yang HH, van Breemen C, Chung AW. Vasomotor dysfunction in the thoracic aorta of Marfan syndrome is associated with accumulation of oxidative stress. Vascul Pharmacol 2010;52:37-45.
7. Vapnik JS, Kim JB, Isselbacher EM, et al. Characteristics and Outcomes of Ascending Versus Descending Thoracic Aortic Aneurysms. Am J Cardiol 2016;117:1683-90.
8. Ostberg NP, Zafar MA, Ziganshin BA, et al. The Genetics of Thoracic Aortic Aneurysms and Dissection: A Clinical Perspective. Biomolecules 2020;10:182.
9. Li Y, Gao S, Han Y, et al. Variants of Focal Adhesion Scaffold Genes Cause Thoracic Aortic Aneurysm. Circ

Res 2021;128:8-23.
10. Prakash SK, LeMaire SA, Guo DC, et al. Rare copy number variants disrupt genes regulating vascular smooth muscle cell adhesion and contractility in sporadic thoracic aortic aneurysms and dissections. Am J Hum Genet 2010;87:743-56.
11. Boileau A, Lino Cardenas CL, Courtois A, et al. MiR-574-5p: A Circulating Marker of Thoracic Aortic Aneurysm. Int J Mol Sci 2019;20:3924.
12. Moushi A, Pillar N, Keravnou A, et al. MicroRNAs in ascending thoracic aortic aneurysms. Biosci Rep 2020;40:BSR20200218.
13. Kakati T, Bhattacharyya DK, Barah P, et al. Comparison of Methods for Differential Co-expression Analysis for Disease Biomarker Prediction. Comput Biol Med 2019;113:103380.
14. Langfelder P, Horvath S. WGCNA: an R package for weighted correlation network analysis. BMC Bioinformatics 2008;9:559.
15. Ma X, Tao R, Li L, et al. Identification of a 5-microRNA signature and hub miRNA-mRNA interactions associated with pancreatic cancer. Oncol Rep 2019;41:292-300.
16. Chen S, Yang D, Lei C, et al. Identification of crucial genes in abdominal aortic aneurysm by WGCNA. PeerJ 2019;7:e7873.
17. Gasiulė S, Stankevičius V, Patamsytė V, et al. Tissue-Specific miRNAs Regulate the Development of Thoracic Aortic Aneurysm: The Emerging Role of KLF4 Network. J Clin Med 2019;8:1609.
18. Bi S, Liu R, He L, et al. Bioinformatics analysis of common key genes and pathways of intracranial, abdominal, and thoracic aneurysms. BMC Cardiovasc Disord 2021;21:14.
19. Santovito D, Weber C. Zooming in on microRNAs for refining cardiovascular risk prediction in secondary prevention. Eur Heart J 2017;38:524-8.
20. Micheau O. Regulation of TNF-Related Apoptosis-Inducing Ligand Signaling by Glycosylation. Int J Mol Sci 2018;19:715.
21. Gonçalves I, Singh P, Tengryd C, et al. sTRAIL-R2 (Soluble TNF [Tumor Necrosis Factor]-Related Apoptosis-Inducing Ligand Receptor 2) a Marker of Plaque Cell Apoptosis and Cardiovascular Events. Stroke 2019;50:1989-96.
22. Huang B, Lu S, Lai H, et al. LncRNA LOXL1-AS is up-regulated in thoracic aortic aneurysm and regulated proliferation and apoptosis of aortic smooth muscle cells. Biosci Rep 2019;39:BSR20191649.
23. Mohammadzadeh A, Mirza-Aghazadeh-Attari M, Hallaj S, et al. Crosstalk between P53 and DNA damage response in ageing. DNA Repair (Amst) 2019;80:8-15.
24. Coutts AS, La Thangue NB. The p53 response: emerging levels of co-factor complexity. Biochem Biophys Res Commun 2005;331:778-85.
25. Zhang WM, Liu Y, Li TT, et al. Sustained activation of ADP/P2ry12 signaling induces SMC senescence contributing to thoracic aortic aneurysm/dissection. J Mol Cell Cardiol 2016;99:76-86.
26. Cao X, Cai Z, Liu J, et al. miRNA504 inhibits p53dependent vascular smooth muscle cell apoptosis and may prevent aneurysm formation. Mol Med Rep 2017;16:2570-8.
27. Leeper NJ, Raiesdana A, Kojima Y, et al. Loss of CDKN2B promotes p53-dependent smooth muscle cell apoptosis and aneurysm formation. Arterioscler Thromb Vasc Biol 2013;33:e1-e10.
28. Kischkel FC, Lawrence DA, Chuntharapai A, et al. Apo2L/TRAIL-dependent recruitment of endogenous FADD and caspase-8 to death receptors 4 and 5. Immunity 2000;12:611-20.
29. Zhang L, Fang B. Mechanisms of resistance to TRAIL-induced apoptosis in cancer. Cancer Gene Ther 2005;12:228-37.
30. Boise LH, González-García M, Postema CE, et al. bcl-x, a bcl-2-related gene that functions as a dominant regulator of apoptotic cell death. Cell 1993;74:597-608.
31. Minn AJ, Boise LH, Thompson CB. Bcl-x(S) anatagonizes the protective effects of Bcl-x(L). J Biol Chem 1996;271:6306-12.
32. Braun T, Dar S, Vorobiov D, et al. Expression of Bcl-x(S) in Xenopus oocytes induces BH3-dependent and caspase-dependent cytochrome c release and apoptosis. Mol Cancer Res 2003;1:186-94.
33. Okura T, Igase M, Kitami Y, et al. Platelet-derived growth factor induces apoptosis in vascular smooth muscle cells: roles of the Bcl-2 family. Biochim Biophys Acta 1998;1403:245-53.
34. Durdu S, Deniz GC, Balci D, et al. Apoptotic vascular smooth muscle cell depletion via BCL2 family of proteins in human ascending aortic aneurysm and dissection. Cardiovasc Ther 2012;30:308-16.
35. Altucci L, Leibowitz MD, Ogilvie KM, et al. RAR and RXR modulation in cancer and metabolic disease. Nat Rev Drug Discov 2007;6:793-810.
36. Grignani F, Ferrucci PF, Testa U, et al. The acute promyelocytic leukemia-specific PML-RAR alpha fusion protein inhibits differentiation and promotes survival of myeloid precursor cells. Cell 1993;74:423-31.

37. Altucci L, Rossin A, Raffelsberger W, et al. Retinoic acid-induced apoptosis in leukemia cells is mediated by paracrine action of tumor-selective death ligand TRAIL. Nat Med 2001;7:680-6.
38. Greiner EF, Kirfel J, Greschik H, et al. Differential ligand-dependent protein-protein interactions between nuclear receptors and a neuronal-specific cofactor. Proc Natl Acad Sci U S A 2000;97:7160-5.
39. Gabriely G, Kama R, Gelin-Licht R, et al. Different domains of the UBL-UBA ubiquitin receptor, Ddi1/Vsm1, are involved in its multiple cellular roles. Mol Biol Cell 2008;19:3625-37.
40. Wen Z, Pan T, Yang S, et al. Up-regulated NRIP2 in colorectal cancer initiating cells modulates the Wnt pathway by targeting RORbeta. Mol Cancer 2017;16:20.
41. Kostina A, Bjork H, Ignatieva E, et al. Notch, BMP and WNT/β-catenin network is impaired in endothelial cells of the patients with thoracic aortic aneurysm. Atheroscler Suppl 2018;35:e6-e13.
42. Krishna SM, Seto SW, Jose RJ, et al. Wnt Signaling Pathway Inhibitor Sclerostin Inhibits Angiotensin II-Induced Aortic Aneurysm and Atherosclerosis. Arterioscler Thromb Vasc Biol 2017;37:553-66.
43. Michel JB. Biology of Vascular Wall Dilation and Rupture: Oxford, UK: Oxford University Press; 2017.
44. Woo CC, Liu W, Lin XY, et al. The interaction between 30b-5p miRNA and MBNL1 mRNA is involved in vascular smooth muscle cell differentiation in patients with coronary atherosclerosis. Int J Mol Sci 2019;21:11.
45. Ji B, Chen L, Cai Q, et al. Identification of an 8-miRNA signature as a potential prognostic biomarker for glioma. PeerJ 2020;8:e9943.
46. Zhuang H, Ma Z, Huang K, et al. Establishment of a 7-miRNA-Based Risk Score System for Predicting Prognosis of Pancreatic Cancer. Pancreas 2020;49:655-62.
47. Wang Y, Barbacioru CC, Shiffman D, et al. Gene expression signature in peripheral blood detects thoracic aortic aneurysm. PLoS One 2007;2:e1050.
48. Gurung R, Choong AM, Woo CC, et al. Genetic and Epigenetic Mechanisms Underlying Vascular Smooth Muscle Cell Phenotypic Modulation in Abdominal Aortic Aneurysm. Int J Mol Sci 2020;21:6334.
49. Goldfinger JZ, Halperin JL, Marin ML, et al. Thoracic aortic aneurysm and dissection. J Am Coll Cardiol 2014;64:1725-39.
50. Zhang L, Wang HH. The genetics and pathogenesis of thoracic aortic aneurysm disorder and dissections. Clin Genet 2016;89:639-46.

(English Language Editors: L. Huleatt and J. Gray)

Cite this article as: Chen S, Ji L, Chen M, Yang D, Zhou J, Zheng Y. Weighted miRNA co-expression network reveals potential roles of apoptosis related pathways and crucial genes in thoracic aortic aneurysm. J Thorac Dis 2021;13(5):2776-2789. doi: 10.21037/jtd-20-3601

Table S1 Functional enrichment of DEMs

Terms	Count	P value	BH method
Biological Process			
Regulation of nucleobase, nucleoside, nucleotide and nucleic acid metabolism	876	1.83E-14	3.26E-12
Signal transduction	1123	2.82E-08	2.51E-06
Cell communication	1037	9.43E-06	0.000559
Regulation of cell growth	13	0.000397	0.017676
Regulation of gene expression, epigenetic	29	0.000678	0.024135
Carbohydrate metabolism	6	0.004384	0.130048
Regulation of cell cycle	23	0.008366	0.212742
Cell organization and biogenesis	5	0.013274	0.228087
Protein modification	10	0.014531	0.228087
Transport	338	0.015945	0.228087
Endosome transport	3	0.015951	0.228087
Morphogenesis	3	0.015951	0.228087
Cell differentiation	13	0.016658	0.228087
Regulation of signal transduction	11	0.022384	0.284592
Regulation of immune response	5	0.028092	0.333361
Hemopoiesis	3	0.051761	0.484916
Peptide metabolism	3	0.051761	0.484916
Neurotransmitter transport	3	0.051761	0.484916
Regulation of development	3	0.051761	0.484916
Chromosome segregation	4	0.072159	0.642216
Regulation of translation	6	0.08253	0.69954
Cell proliferation	14	0.090172	0.729574
Apoptosis	64	0.103669	0.779986
Cell motility	8	0.105167	0.779986
Protein transport	5	0.117415	0.835997
Cellular morphogenesis during differentiation	2	0.158225	0.901539
Intracellular signaling cascade	2	0.158225	0.901539
Regulation of cellular process	2	0.158225	0.901539
Steroid metabolism	2	0.158225	0.901539
Transcription	15	0.160033	0.901539
Fatty acid metabolism	5	0.16124	0.901539
Organogenesis	4	0.168989	0.901539
Development	3	0.172204	0.901539
Electron transport	3	0.172204	0.901539
Lipid metabolism	11	0.187287	0.923821
Cell development	5	0.210433	0.923821
Nucleobase, nucleoside, nucleotide and nucleic acid transport	3	0.247238	0.923821
Immune cell migration	1	0.251766	0.923821
Lymphocyte proliferation	1	0.251766	0.923821
Lymphocyte activation	1	0.251766	0.923821
Phosphoinositide-mediated signaling	1	0.251766	0.923821
Antigen presentation	1	0.251766	0.923821
Learning and/or memory	1	0.251766	0.923821
Plasma membrane organization and biogenesis	1	0.251766	0.923821
Enzyme linked receptor protein signaling pathway	1	0.251766	0.923821
Regulation of hormone secretion	1	0.251766	0.923821
Regulation of viral life cycle	1	0.251766	0.923821
Cytoskeleton organization and biogenesis	7	0.262556	0.923821
Cell fate commitment	2	0.26469	0.923821
Skeletal development	2	0.26469	0.923821
Cytokine and chemokine mediated signaling pathway	2	0.26469	0.923821
Anti-apoptosis	10	0.27099	0.92762
Cell surface receptor linked signal transduction	3	0.325845	1
Regulation of cell proliferation	7	0.353651	1
Cell-cell adhesion	4	0.356676	1
Regulation of metabolism	2	0.370912	1
Regulation of exocytosis	2	0.370912	1
Mitosis	2	0.370912	1
Regulation of enzyme activity	2	0.370912	1
Mitochondrial transport	2	0.370912	1
Protein targeting	2	0.370912	1
Carbohydrate mediated signaling	1	0.440156	1
Steroid hormone receptor signaling pathway	1	0.440156	1
CAMP-mediated signaling	1	0.440156	1
RNA localization	1	0.440156	1
Cell death	2	0.470266	1
Cell cycle	6	0.490964	1
Protein metabolism	332	0.53972	1
Cell migration	4	0.545112	1
Lipid transport	2	0.559478	1
Neurogenesis	2	0.559478	1
Wound healing	1	0.581121	1
Bone remodeling	1	0.581121	1
Amino acid transport	1	0.581121	1
Signal complex formation	1	0.581121	1
Gene silencing	1	0.581121	1
Protein localization	1	0.581121	1
Hormone metabolism	1	0.581121	1
Cell adhesion	13	0.625591	1
Vesicle-mediated transport	4	0.653291	1
Cell growth and/or maintenance	278	0.656359	1
RNA metabolism	6	0.670515	1
Amino acid and derivative metabolism	1	0.686598	1
Cytoskeletal anchoring	1	0.686598	1
Regulation of endocytosis	1	0.686598	1
Vesicle docking	1	0.686598	1
Ribosome biogenesis and assembly	1	0.686598	1
Innate immune response	1	0.686598	1
Cell recognition	1	0.686598	1
Ion transport	11	0.693821	1
G-protein coupled receptor protein signaling pathway	2	0.760006	1
Microtubule-based process	1	0.765519	1
Regulation of physiological process	1	0.765519	1
Embryonic development	2	0.806608	1
Protein folding	3	0.807377	1
Proteolysis and peptidolysis	3	0.807377	1
Cell-cell signaling	3	0.807377	1
DNA replication	2	0.876266	1
DNA repair	11	0.896196	1
Calcium-mediated signaling	1	0.92654	1
Metabolism	338	1	1
Energy pathways	320	1	1
Immune response	59	1	1
Biological_process unknown	1009	1	1
Biological Pathways			
Glypican pathway	532	4.98E-30	4.83E-27
Proteoglycan syndecan-mediated signaling events	534	5.79E-30	4.83E-27
TRAIL signaling pathway	527	2E-29	9.03E-27
Syndecan-1-mediated signaling events	518	2.29E-29	9.03E-27
ErbB receptor signaling network	521	3.25E-29	9.03E-27
Sphingosine 1-phosphate (S1P) pathway	521	3.25E-29	9.03E-27
Beta1 integrin cell surface interactions	533	4.96E-29	1.14E-26
VEGF and VEGFR signaling network	518	5.88E-29	1.14E-26
Plasma membrane estrogen receptor signaling	517	6.13E-29	1.14E-26
Alpha9 beta1 integrin signaling events	518	7.44E-29	1.24E-26
Signaling events mediated by Hepatocyte Growth Factor Receptor (c-Met)	514	8.75E-29	1.33E-26
Signaling events mediated by VEGFR1 and VEGFR2	514	1.77E-28	2.36E-26
PDGF receptor signaling network	513	1.84E-28	2.36E-26
IGF1 pathway	512	2.42E-28	2.75E-26
Nectin adhesion pathway	513	2.93E-28	2.75E-26
IL5-mediated signaling events	512	3.05E-28	2.75E-26
Glypican 1 network	514	3.55E-28	2.75E-26
IFN-gamma pathway	513	3.7E-28	2.75E-26
EGF receptor (ErbB1) signaling pathway	510	5.27E-28	2.75E-26
Signaling events mediated by focal adhesion kinase	510	5.27E-28	2.75E-26
Arf6 downstream pathway	510	5.27E-28	2.75E-26
Internalization of ErbB1	510	5.27E-28	2.75E-26
Insulin Pathway	510	5.27E-28	2.75E-26
Urokinase-type plasminogen activator (uPA) and uPAR-mediated signaling	510	5.27E-28	2.75E-26
S1P1 pathway	510	5.27E-28	2.75E-26
Class I PI3K signaling events	510	5.27E-28	2.75E-26
PDGFR-beta signaling pathway	510	5.27E-28	2.75E-26
Arf6 signaling events	510	5.27E-28	2.75E-26
ErbB1 downstream signaling	510	5.27E-28	2.75E-26
Arf6 trafficking events	510	5.27E-28	2.75E-26
Class I PI3K signaling events mediated by Akt	510	5.27E-28	2.75E-26
mTOR signaling pathway	510	5.27E-28	2.75E-26
GMCSF-mediated signaling events	511	6.38E-28	3.22E-26
EGFR-dependent Endothelin signaling events	510	6.64E-28	3.26E-26
Integrin family cell surface interactions	537	1.25E-27	5.9E-26
IL3-mediated signaling events	511	1.27E-27	5.9E-26
Endothelins	514	2.23E-27	1E-25
LKB1 signaling events	514	2.8E-27	1.23E-25
PAR1-mediated thrombin signaling events	511	3.17E-27	1.36E-25
Thrombin/protease-activated receptor (PAR) pathway	511	3.98E-27	1.66E-25
Regulation of CDC42 activity	321	7.71E-21	3.14E-19
CDC42 signaling events	316	1.31E-20	5.18E-19
Integrin-linked kinase signaling	282	1.48E-20	5.76E-19
AP-1 transcription factor network	270	2.84E-20	1.08E-18
TGF-beta receptor signaling	148	3.74E-16	1.33E-14
Regulation of nuclear SMAD2/3 signaling	148	3.74E-16	1.33E-14
Regulation of cytoplasmic and nuclear SMAD2/3 signaling	148	3.74E-16	1.33E-14
ALK1 signaling events	153	8.57E-16	2.98E-14
ALK1 pathway	154	9.34E-16	3.18E-14
TGFBR	69	2.61E-11	8.7E-10
BMP receptor signaling	104	5.89E-10	1.93E-08
TNF receptor signaling pathway	126	8.71E-09	2.79E-07
Signaling by EGFR	53	1.41E-08	4.45E-07
p38 MAPK signaling pathway	86	3.62E-08	1.12E-06
Regulation of p38-alpha and p38-beta	76	8.95E-08	2.72E-06
IL1-mediated signaling events	99	2.9E-07	8.65E-06
Wnt signaling network	87	3.65E-07	1.07E-05
EGFR1	65	3.7E-07	1.07E-05
Glypican 3 network	89	3.87E-07	1.1E-05
N-cadherin signaling events	104	4.96E-07	1.38E-05
NGF signalling via TRKA from the plasma membrane	53	6.27E-07	1.69E-05
EPHB forward signaling	26	6.28E-07	1.69E-05
Syndecan-4-mediated signaling events	89	8.34E-07	2.21E-05
Neurotrophic factor-mediated Trk receptor signaling	50	1.33E-06	3.46E-05
Epithelial-to-mesenchymal transition	79	3.04E-06	7.81E-05
Signalling by NGF	64	4.11E-06	0.000104
p75(NTR)-mediated signaling	76	4.71E-06	0.000116
EphrinB-EPHB pathway	33	4.74E-06	0.000116
Trk receptor signaling mediated by the MAPK pathway	22	5.23E-06	0.000126
Trk receptor signaling mediated by PI3K and PLC-gamma	34	5.99E-06	0.000143
Noncanonical Wnt signaling pathway	77	6.16E-06	0.000145
Posttranslational regulation of adherens junction stability and dissassembly	93	8.54E-06	0.000196
Axon guidance	89	8.58E-06	0.000196
Stabilization and expansion of the E-cadherin adherens junction	107	1.12E-05	0.00025
E-cadherin signaling in the nascent adherens junction	107	1.12E-05	0.00025
CXCR4-mediated signaling events	78	2.01E-05	0.000424
Regulation of RhoA activity	83	2.03E-05	0.000424
RAC1 signaling pathway	83	2.03E-05	0.000424
RhoA signaling pathway	83	2.03E-05	0.000424
Regulation of RAC1 activity	83	2.03E-05	0.000424
Regulation of retinoblastoma protein	34	2.25E-05	0.000463
Wnt	40	2.35E-05	0.000478
E-cadherin signaling events	107	2.8E-05	0.000563
Notch signaling pathway	44	3.43E-05	0.000674
Notch-mediated HES/HEY network	44	3.43E-05	0.000674
AndrogenReceptor	38	3.88E-05	0.000753
Canonical Wnt signaling pathway	65	4.5E-05	0.000863
Signaling by FGFR	44	4.73E-05	0.000897
Regulation of nuclear beta catenin signaling and target gene transcription	58	5.03E-05	0.000943
TCR signaling in naïve CD4+ T cells	57	6.34E-05	0.001174
Insulin receptor signalling cascade	29	7.9E-05	0.001448
IRS-mediated signalling	27	8.46E-05	0.001533
DARPP-32 events	13	8.88E-05	0.001592
Downstream signal transduction	36	9.14E-05	0.001621
ATF-2 transcription factor network	30	9.28E-05	0.001629
Signaling by PDGF	37	0.0001	0.001743
HIF-2-alpha transcription factor network	20	0.000103	0.001773
IL2-mediated signaling events	50	0.000114	0.001936
Signaling events mediated by Stem cell factor receptor (c-Kit)	27	0.000131	0.002203
Signalling to ERKs	18	0.000162	0.002695
Downstream signaling of activated FGFR	32	0.000175	0.002863
Signaling by SCF-KIT	32	0.000175	0.002863
IRS-related events	27	0.000198	0.003209
Integrins in angiogenesis	31	0.000225	0.003612
Role of Calcineurin-dependent NFAT signaling in lymphocytes	42	0.000253	0.004023
SOS-mediated signalling	11	0.000261	0.004109
EPHA forward signaling	18	0.000288	0.004486
Developmental Biology	149	0.000355	0.005484
VEGFR1 specific signals	17	0.000363	0.005562
Retinoic acid receptors-mediated signaling	24	0.000425	0.006438
EGFR downregulation	16	0.000458	0.00688
Signaling mediated by p38-alpha and p38-beta	25	0.00049	0.007256
Netrin-mediated signaling events	18	0.000492	0.007256
Growth hormone receptor signaling	12	0.000539	0.007894
VEGFR3 signaling in lymphatic endothelium	15	0.000575	0.008337
EphrinA-EPHA pathway	22	0.000707	0.010173
ErbB2/ErbB3 signaling events	20	0.000771	0.01099
FoxO family signaling	24	0.000924	0.013057
Syndecan-2-mediated signaling events	34	0.000981	0.013744
NOD1/2 Signaling Pathway	15	0.001019	0.014163
G1 Phase	17	0.00104	0.014218
Cyclin D associated events in G1	17	0.00104	0.014218
Frs2-mediated activation	12	0.001103	0.014952
EPO signaling pathway	18	0.001285	0.01729
S1P3 pathway	16	0.001338	0.017848
JNK signaling in the CD4+ TCR pathway	21	0.001365	0.017946
Membrane Trafficking	36	0.001366	0.017946
FRS2-mediated cascade	10	0.00162	0.020946
GRB2 events in EGFR signaling	10	0.00162	0.020946
MyD88 cascade initiated on plasma membrane	27	0.001671	0.021279
TRAF6 mediated induction of NFkB and MAP kinases upon TLR7/8 or 9 activation	27	0.001671	0.021279
L1CAM interactions	34	0.001684	0.021279
Signaling by TGF beta	9	0.001906	0.02372
SHC-mediated signalling	9	0.001906	0.02372
Prolonged ERK activation events	12	0.002077	0.025666
MAP kinase activation in TLR cascade	16	0.002149	0.026164
PLC-gamma1 signalling	16	0.002149	0.026164
MyD88 dependent cascade initiated on endosome	27	0.002263	0.026965
Toll Like Receptor 5 (TLR5) Cascade	27	0.002263	0.026965
Toll Like Receptor 10 (TLR10) Cascade	27	0.002263	0.026965
Signaling events mediated by TCPTP	38	0.002295	0.027149
Ceramide signaling pathway	23	0.002402	0.028213
Transcriptional Regulation of White Adipocyte Differentiation	30	0.002553	0.029782
Validated targets of C-MYC transcriptional activation	34	0.002788	0.03229
Signaling events mediated by PRL	13	0.002845	0.032722
IL6-mediated signaling events	22	0.003095	0.035363
Androgen-mediated signaling	50	0.003204	0.035883
BCR signaling pathway	29	0.00324	0.035883
Platelet calcium homeostasis	10	0.00327	0.035883
Signalling to p38 via RIT and RIN	10	0.00327	0.035883
Regulation of Insulin Secretion by Glucagon-like Peptide-1	10	0.00327	0.035883
SHC1 events in EGFR signaling	10	0.00327	0.035883
RXR and RAR heterodimerization with other nuclear receptor	14	0.003605	0.039044
S1P2 pathway	14	0.003605	0.039044
Signalling to RAS	12	0.003656	0.039338
Ras signaling in the CD4+ TCR pathway	20	0.00368	0.039352
MyD88:Mal cascade initiated on plasma membrane	27	0.003993	0.041893
Toll Like Receptor 7/8 (TLR7/8) Cascade	27	0.003993	0.041893
IL4-mediated signaling events	27	0.003993	0.041893
Toll Like Receptor 9 (TLR9) Cascade	28	0.00411	0.042842
EGFR interacts with phospholipase C-gamma	15	0.00433	0.044857
Signaling by BMP	11	0.004694	0.047738
Citric acid cycle (TCA cycle)	11	0.004694	0.047738
PKA activation	11	0.004694	0.047738
KitReceptor	24	0.004731	0.047829
ERK/MAPK targets	8	0.004943	0.049664
Circadian Clock	16	0.005003	0.049967
Beta3 integrin cell surface interactions	20	0.005148	0.051115
Signaling events regulated by Ret tyrosine kinase	29	0.005406	0.053357
FAS (CD95) signaling pathway	49	0.005563	0.054323
Signal transduction by L1	17	0.005615	0.054323
Phospholipase C-mediated cascade	14	0.005634	0.054323
DAG and IP3 signaling	14	0.005634	0.054323
C-MYC pathway	55	0.005717	0.054807
Activation of BH3-only proteins	10	0.006018	0.057357
PI3K Cascade	18	0.006162	0.058402
Aurora B signaling	19	0.006645	0.062619
Toll Like Receptor TLR1:TLR2 Cascade	27	0.00672	0.062619
Toll Like Receptor TLR6:TLR2 Cascade	27	0.00672	0.062619
E2F transcription factor network	30	0.006921	0.064032
Signaling by Insulin receptor	32	0.006948	0.064032
Clathrin derived vesicle budding	16	0.007295	0.066489
trans-Golgi Network Vesicle Budding	16	0.007295	0.066489
Lysosome Vesicle Biogenesis	9	0.007696	0.068966
CREB phosphorylation through the activation of CaMKII	9	0.007696	0.068966
Nuclear Events (kinase and transcription factor activation)	9	0.007696	0.068966
TRAF6 Mediated Induction of proinflammatory cytokines	22	0.007732	0.068966
PKA-mediated phosphorylation of CREB	11	0.007892	0.070016
Signaling by Aurora kinases	38	0.008115	0.071622
Toll Like Receptor 2 (TLR2) Cascade	27	0.008575	0.075276
Hypoxic and oxygen homeostasis regulation of HIF-1-alpha	32	0.008623	0.075305
FOXM1 transcription factor network	19	0.009095	0.079009
Regulation of Androgen receptor activity	41	0.00927	0.080115
G alpha (s) signalling events	15	0.00949	0.080763
Intrinsic Pathway for Apoptosis	15	0.00949	0.080763
Pyruvate metabolism and Citric Acid (TCA) cycle	15	0.00949	0.080763
Signaling by Robo receptor	12	0.00959	0.080788
heparan sulfate biosynthesis	12	0.00959	0.080788
N-glycan trimming in the ER and Calnexin/Calreticulin cycle	8	0.009802	0.082157
ARMS-mediated activation	10	0.010272	0.085664
NFkB and MAP kinases activation mediated by TLR4 signaling repertoire	23	0.010401	0.08631
NOTCH	24	0.010575	0.086894
NCAM signaling for neurite out-growth	24	0.010575	0.086894
p73 transcription factor network	31	0.010706	0.087536
Activated TLR4 signalling	29	0.01082	0.088037
p53 pathway	66	0.011226	0.090895
Direct p53 effectors	50	0.012107	0.097556
Calcium signaling in the CD4+ TCR pathway	14	0.012366	0.098437
RAF/MAP kinase cascade	7	0.012393	0.098437
Signal attenuation	7	0.012393	0.098437
Calcineurin-regulated NFAT-dependent transcription in lymphocytes	21	0.012951	0.102379
SHC-related events	9	0.013387	0.104628
ErbB4 signaling events	15	0.01345	0.104628
Recycling pathway of L1	15	0.01345	0.104628
MyD88-independent cascade initiated on plasma membrane	24	0.013487	0.104628
Coregulation of Androgen receptor activity	25	0.013549	0.104628
pyrimidine ribonucleotides interconversion	6	0.015463	0.118315
Regulation of KIT signaling	6	0.015463	0.118315
Golgi Associated Vesicle Biogenesis	13	0.016142	0.121831
Ca-dependent events	13	0.016142	0.121831
mTOR signalling	13	0.016142	0.121831
TCR signaling	20	0.016482	0.123837
Angiopoietin receptor Tie2-mediated signaling	21	0.01673	0.125138
Opioid Signalling	22	0.016892	0.125323
Toll Like Receptor 3 (TLR3) Cascade	23	0.01698	0.125323
TRIF mediated TLR3 signaling	23	0.01698	0.125323
Synthesis of very long-chain fatty acyl-CoAs	8	0.01747	0.12725
S1P4 pathway	8	0.01747	0.12725
guanosine nucleotides de novo biosynthesis	8	0.01747	0.12725
C-MYB transcription factor network	32	0.01895	0.13683
Deadenylation of mRNA	11	0.019031	0.13683
Cellular roles of Anthrax toxin	11	0.019031	0.13683
Factors involved in megakaryocyte development and platelet production	43	0.019945	0.141379
ERK1 activation	3	0.020173	0.141379
Cam-PDE 1 activation	3	0.020173	0.141379
Binding of RNA by Insulin-like Growth Factor-2 mRNA Binding Proteins (IGF2BPs/IMPs/VICKZs)	3	0.020173	0.141379
p75NTR negatively regulates cell cycle via SC1	3	0.020173	0.141379
ERKs are inactivated	3	0.020173	0.141379
HIF-1-alpha transcription factor network	26	0.020833	0.145393
Calmodulin induced events	12	0.021115	0.145494
CaM pathway	12	0.021115	0.145494
Alpha6Beta4Integrin	20	0.021196	0.145494
FGF signaling pathway	20	0.021196	0.145494
Botulinum neurotoxicity	4	0.021467	0.146389
Negative regulation of FGFR signaling	9	0.021677	0.146389
PKA activation in glucagon signalling	9	0.021677	0.146389
Ras activation uopn Ca2+ infux through NMDA receptor	9	0.021677	0.146389
CREB phosphorylation through the activation of Ras	13	0.022777	0.151675
IL2 signaling events mediated by STAT5	13	0.022777	0.151675
PKB-mediated events	13	0.022777	0.151675
Calnexin/calreticulin cycle	7	0.022824	0.151675
Lissencephaly gene (LIS1) in neuronal migration and development	14	0.024077	0.15916
Toll Like Receptor 4 (TLR4) Cascade	29	0.024141	0.15916
Activation of NMDA receptor upon glutamate binding and postsynaptic events	15	0.02507	0.163988
Post NMDA receptor activation events	15	0.02507	0.163988
Signaling by Interleukins	34	0.025592	0.166748
Hemostasis	119	0.026308	0.169505
Platelet homeostasis	17	0.02632	0.169505
G-protein mediated events	17	0.02632	0.169505
Signaling events mediated by PTP1B	21	0.026825	0.172094
BMAL1:CLOCK/NPAS2 Activates Gene Expression	11	0.027686	0.176262
APC-Cdc20 mediated degradation of Nek2A	11	0.027686	0.176262
Adaptive Immune System	78	0.028583	0.181278
Rap1 signalling	6	0.029834	0.187782
Reduction of cytosolic Ca++ levels	6	0.029834	0.187782
TNF alpha/NF-kB	58	0.030384	0.190526
Reelin signaling pathway	13	0.031235	0.195134
Tie2 Signaling	9	0.033083	0.205306
a6b1 and a6b4 Integrin signaling	15	0.03311	0.205306
ATM pathway	98	0.035362	0.218458
MAPK targets/ Nuclear events mediated by MAP kinases	10	0.036407	0.221628
PDGFR-alpha signaling pathway	10	0.036407	0.221628
Trafficking of AMPA receptors	10	0.036407	0.221628
Glutamate Binding, Activation of AMPA Receptors and Synaptic Plasticity	10	0.036407	0.221628
TCR signaling in naïve CD8+ T cells	44	0.038614	0.234209
Role of DCC in regulating apoptosis	5	0.03895	0.235393
Validated transcriptional targets of AP1 family members Fra1 and Fra2	46	0.040866	0.24608
PI3K/AKT activation	13	0.041747	0.250483
Regulation of Insulin Secretion	19	0.042149	0.251557
Glucagon signaling in metabolic regulation	14	0.042484	0.251557
Alpha4 beta1 integrin signaling events	14	0.042484	0.251557
Netrin-1 signaling	18	0.04258	0.251557
p63 transcription factor network	37	0.042775	0.251557
Interleukin-1 signaling	16	0.042982	0.251557
PLC beta mediated events	16	0.042982	0.251557
Cell-extracellular matrix interactions	8	0.043894	0.25334
phosphatidylglycerol biosynthesis II (non-plastidic)	8	0.043894	0.25334
Spry regulation of FGF signaling	8	0.043894	0.25334
heparan sulfate biosynthesis (late stages)	8	0.043894	0.25334
Apoptosis	53	0.045312	0.26062
Polo-like kinase signaling events in the cell cycle	38	0.047368	0.271512
Fc-epsilon receptor I signaling in mast cells	23	0.047588	0.271836
EPHA2 forward signaling	9	0.048036	0.273462
ERK activation	4	0.050555	0.279202
activated TAK1 mediates p38 MAPK activation	4	0.050555	0.279202
SHC-mediated cascade	4	0.050555	0.279202
Elevation of cytosolic Ca2+ levels	4	0.050555	0.279202
Regulation of gene expression in early pancreatic precursor cells	4	0.050555	0.279202
S6K1-mediated signalling	6	0.050762	0.279202
Unblocking of NMDA receptor, glutamate binding and activation	6	0.050762	0.279202
pyrimidine ribonucleotides de novo biosynthesis	6	0.050762	0.279202
mTORC1-mediated signalling	6	0.050762	0.279202
Mitotic Metaphase/Anaphase Transition	10	0.050886	0.279202
APC/C:Cdc20 mediated degradation of Cyclin B	10	0.050886	0.279202
Cleavage of Growing Transcript in the Termination Region	17	0.053473	0.289587
Nucleotide-binding domain, leucine rich repeat containing receptor (NLR) signaling pathways	17	0.053473	0.289587
RNA Polymerase II Transcription Termination	17	0.053473	0.289587
Post-Elongation Processing of the Transcript	17	0.053473	0.289587
Endosomal Sorting Complex Required For Transport (ESCRT)	12	0.053917	0.291045
CXCR3-mediated signaling events	15	0.054509	0.293295
Cyclin E associated events during G1/S transition	28	0.057399	0.30785
PLK1 signaling events	36	0.057889	0.309482
Class I MHC mediated antigen processing & presentation	35	0.059957	0.319516
Integrin cell surface interactions	26	0.06118	0.324995
Glucocorticoid receptor signaling	30	0.062219	0.329467
Activation of PUMA and translocation to mitochondria	3	0.064231	0.33376
NADE modulates death signalling	3	0.064231	0.33376
Neurophilin interactions with VEGF and VEGFR	3	0.064231	0.33376
Localization of the PINCH-ILK-PARVIN complex to focal adhesions	3	0.064231	0.33376
Activation of NOXA and translocation to mitochondria	3	0.064231	0.33376
arginine degradation I (arginase pathway)	3	0.064231	0.33376
Effects of PIP2 hydrolysis	9	0.066846	0.346106
Serotonin Neurotransmitter Release Cycle	5	0.068308	0.346106
glycerol degradation I	5	0.068308	0.346106
Dopamine Neurotransmitter Release Cycle	5	0.068308	0.346106
Sodium/Calcium exchangers	5	0.068308	0.346106
Regulation of pyruvate dehydrogenase (PDH) complex	5	0.068308	0.346106
Nef mediated downregulation of MHC class I complex cell surface expression	5	0.068308	0.346106
Receptor-ligand binding initiates the second proteolytic cleavage of Notch receptor	5	0.068308	0.346106
Antigen Presentation: Folding, assembly and peptide loading of class I MHC	10	0.068731	0.346106
Neurotransmitter Receptor Binding And Downstream Transmission In The Postsynaptic Cell	31	0.069035	0.346106
Downstream TCR signaling	13	0.069675	0.346106
GAB1 signalosome	13	0.069675	0.346106
Insulin-mediated glucose transport	12	0.069927	0.346106
Nephrin interactions	12	0.069927	0.346106
Sphingolipid metabolism	12	0.069927	0.346106
Osteopontin-mediated events	12	0.069927	0.346106
Integration of energy metabolism	29	0.074101	0.355341
Transcriptional activation of cell cycle inhibitor p21	2	0.074136	0.355341
FGFR2c ligand binding and activation	2	0.074136	0.355341
FGFR3c ligand binding and activation	2	0.074136	0.355341
FGFR3b ligand binding and activation	2	0.074136	0.355341
FGFR3 ligand binding and activation	2	0.074136	0.355341
Assembly of Viral Components at the Budding Site	2	0.074136	0.355341
Virus Assembly and Release	2	0.074136	0.355341
Inhibition of Host mRNA Processing and RNA Silencing	2	0.074136	0.355341
Translocation of BoNT Light chain	2	0.074136	0.355341
Transcriptional activation of p53 responsive genes	2	0.074136	0.355341
SCF(Skp2)-mediated degradation of p27/p21	24	0.076228	0.363282
IL2 signaling events mediated by PI3K	24	0.076228	0.363282
Glucocorticoid receptor regulatory network	28	0.076778	0.36486
Signaling events mediated by HDAC Class I	38	0.077792	0.368629
Hormone-sensitive lipase (HSL)-mediated triacylglycerol hydrolysis	6	0.0787	0.370822
Tetrahydrobiopterin (BH4) synthesis, recycling, salvage and regulation	6	0.0787	0.370822
LPA receptor mediated events	34	0.080071	0.376219
Cell-Cell communication	39	0.083962	0.393396
CDP-diacylglycerol biosynthesis I	7	0.084746	0.395955
Neuronal System	60	0.085166	0.396806
Inactivation of APC/C via direct inhibition of the APC/C complex	8	0.088089	0.40366
Activated AMPK stimulates fatty-acid oxidation in muscle	8	0.088089	0.40366
Na+/Cl- dependent neurotransmitter transporters	8	0.088089	0.40366
Phosphorylation of the APC/C	8	0.088089	0.40366
Fatty Acyl-CoA Biosynthesis	8	0.088089	0.40366
Inhibition of the proteolytic activity of APC/C required for the onset of anaphase by mitotic spindle checkpoint components	8	0.088089	0.40366
G alpha (12/13) signalling events	9	0.089675	0.405008
p38 signaling mediated by MAPKAP kinases	9	0.089675	0.405008
Aquaporin-mediated transport	11	0.08968	0.405008
Sema4D in semaphorin signaling	11	0.08968	0.405008
CDO in myogenesis	10	0.090083	0.405008
Myogenesis	10	0.090083	0.405008
Regulation of Water Balance by Renal Aquaporins	10	0.090083	0.405008
Signaling events mediated by the Hedgehog family	23	0.091741	0.409976
JNK (c-Jun kinases) phosphorylation and activation mediated by activated human TAK1	4	0.092908	0.409976
FGFR2b ligand binding and activation	4	0.092908	0.409976
RAF phosphorylates MEK	4	0.092908	0.409976
FGFR2 ligand binding and activation	4	0.092908	0.409976
MEK activation	4	0.092908	0.409976
glycoaminoglycan-protein linkage region biosynthesis	4	0.092908	0.409976
Ion channel transport	17	0.095776	0.420405
Deadenylation-dependent mRNA decay	17	0.095776	0.420405
Regulation of Rheb GTPase activity by AMPK	5	0.106783	0.461437
IRAK1 recruits IKK complex	5	0.106783	0.461437
IRAK1 recruits IKK complex upon TLR7/8 or 9 stimulation	5	0.106783	0.461437
Role of second messengers in netrin-1 signaling	5	0.106783	0.461437
GRB2:SOS provides linkage to MAPK signaling for Intergrins	5	0.106783	0.461437
Pyruvate metabolism	5	0.106783	0.461437
mRNA 3'-end processing	13	0.107578	0.462474
Post-Elongation Processing of Intron-Containing pre-mRNA	13	0.107578	0.462474
ATR signaling pathway	77	0.112049	0.480457
Transport to the Golgi and subsequent modification	11	0.112821	0.482527
Conversion from APC/C:Cdc20 to APC/C:Cdh1 in late anaphase	7	0.116519	0.493329
Regulation of AMPK activity via LKB1	7	0.116519	0.493329
LPA4-mediated signaling events	7	0.116519	0.493329
Sema4D induced cell migration and growth-cone collapse	9	0.11653	0.493329
Mitotic Spindle Checkpoint	8	0.117218	0.494986
Toll Receptor Cascades	30	0.118204	0.496635
Cyclin A:Cdk2-associated events at S phase entry	30	0.118204	0.496635
Asparagine N-linked glycosylation	26	0.122756	0.508627
Aurora A signaling	22	0.126389	0.508627
Semaphorin interactions	22	0.126389	0.508627
Validated transcriptional targets of deltaNp63 isoforms	22	0.126389	0.508627
Transmission across Chemical Synapses	39	0.127137	0.508627
Activation of CaMK IV	3	0.128376	0.508627
Synthesis of UDP-N-acetyl-glucosamine	3	0.128376	0.508627
CaMK IV-mediated phosphorylation of CREB	3	0.128376	0.508627
Host Interactions with Influenza Factors	3	0.128376	0.508627
Gap junction trafficking	3	0.128376	0.508627
Electric Transmission Across Gap Junctions	3	0.128376	0.508627
GABA A receptor activation	3	0.128376	0.508627
Regulation of gene expression in endocrine-committed (NEUROG3+) progenitor cells	3	0.128376	0.508627
Signaling by VEGF	3	0.128376	0.508627
VEGF ligand-receptor interactions	3	0.128376	0.508627
S6K1 signalling	3	0.128376	0.508627
Axonal growth stimulation	3	0.128376	0.508627
CHL1 interactions	3	0.128376	0.508627
UDP-N-acetyl-D-glucosamine biosynthesis II	3	0.128376	0.508627
Activation of BIM and translocation to mitochondria	3	0.128376	0.508627
RAF activation	3	0.128376	0.508627
FasL/ CD95L signaling	3	0.128376	0.508627
Transmission across Electrical Synapses	3	0.128376	0.508627
AMPK inhibits chREBP transcriptional activation activity	3	0.128376	0.508627
HIV-1 Nef: Negative effector of Fas and TNF-alpha	13	0.130344	0.515199
Ion transport by P-type ATPases	11	0.139034	0.548249
Nongenotropic Androgen signaling	10	0.143264	0.563596
Regulation of Apoptosis	25	0.144203	0.564455
Activation of Rac	4	0.146867	0.564455
p75NTR regulates axonogenesis	4	0.146867	0.564455
Import of palmitoyl-CoA into the mitochondrial matrix	4	0.146867	0.564455
Regulation of cytoskeletal remodeling and cell spreading by IPP complex components	4	0.146867	0.564455
Notch receptor binds with a ligand	4	0.146867	0.564455
S1P5 pathway	4	0.146867	0.564455
Rho GTPase cycle	4	0.146867	0.564455
Signaling by Rho GTPases	4	0.146867	0.564455
Interleukin-6 signaling	4	0.146867	0.564455
NCAM1 interactions	9	0.147257	0.564655
Costimulation by the CD28 family	18	0.148405	0.567752
Destabilization of mRNA by Butyrate Response Factor 1 (BRF1)	8	0.150799	0.56908
Nef-mediates down modulation of cell surface receptors by recruiting them to clathrin adapters	8	0.150799	0.56908
chondroitin sulfate biosynthesis	8	0.150799	0.56908
superpathway of D-myo-inositol (1,4,5)-trisphosphate metabolism	8	0.150799	0.56908
Integrin alphaIIb beta3 signaling	8	0.150799	0.56908
Phosphorylation of Emi1	8	0.150799	0.56908
Formation and Maturation of mRNA Transcript	57	0.152632	0.569098
ALK2 signaling events	5	0.153468	0.569098
Norepinephrine Neurotransmitter Release Cycle	5	0.153468	0.569098
dermatan sulfate biosynthesis	7	0.153534	0.569098
Beta5 beta6 beta7 and beta8 integrin cell surface interactions	7	0.153534	0.569098
Energy dependent regulation of mTOR by LKB1-AMPK	7	0.153534	0.569098
GABA synthesis, release, reuptake and degradation	7	0.153534	0.569098
Destabilization of mRNA by Tristetraprolin (TTP)	7	0.153534	0.569098
NRIF signals cell death from the nucleus	6	0.154826	0.57009
ID	6	0.154826	0.57009
pyrimidine deoxyribonucleotides de novo biosynthesis	6	0.154826	0.57009
CD28 co-stimulation	13	0.155573	0.571577
Cell junction organization	23	0.156529	0.573826
Antigen processing-Cross presentation	28	0.159732	0.584284
Presenilin action in Notch and Wnt signaling	16	0.161188	0.588319
G1/S DNA Damage Checkpoints	25	0.161868	0.589509
Ephrin B reverse signaling	11	0.168168	0.61112
Immune System	152	0.168642	0.61148
mRNA Splicing - Major Pathway	34	0.169367	0.61148
mRNA Splicing	34	0.169367	0.61148
Platelet activation, signaling and aggregation	43	0.170453	0.614073
ER-Phagosome pathway	26	0.173334	0.623106
The role of Nef in HIV-1 replication and disease pathogenesis	10	0.174784	0.625623
PI-3K cascade	10	0.174784	0.625623
Regulation of mRNA Stability by Proteins that Bind AU-rich Elements	33	0.176118	0.626144
Smooth Muscle Contraction	9	0.181562	0.626144
Autointegration results in viral DNA circles	2	0.182062	0.626144
Class IB PI3K non-lipid kinase events	2	0.182062	0.626144
Proteolytic cleavage of SNARE complex proteins	2	0.182062	0.626144
Formation of the active cofactor, UDP-glucuronate	2	0.182062	0.626144
NFG and proNGF binds to p75NTR	2	0.182062	0.626144
NS1 Mediated Effects on Host Pathways	2	0.182062	0.626144
TWIK related potassium channel (TREK)	2	0.182062	0.626144
tetrahydrobiopterin biosynthesis II	2	0.182062	0.626144
BH3-only proteins associate with and inactivate anti-apoptotic BCL-2 members	2	0.182062	0.626144
Ceramide signalling	2	0.182062	0.626144
D-myo-inositol (1,4,5,6)-tetrakisphosphate biosynthesis	2	0.182062	0.626144
Signalling to STAT3	2	0.182062	0.626144
G2 Phase	2	0.182062	0.626144
tetrahydrobiopterin biosynthesis I	2	0.182062	0.626144
Progressive trimming of alpha-1,2-linked mannose residues from Man9/8/7GlcNAc2 to produce Man5GlcNAc2	2	0.182062	0.626144
Arachidonate production from DAG	2	0.182062	0.626144
Ephrin A reverse signaling	2	0.182062	0.626144
Cell death signalling via NRAGE, NRIF and NADE	8	0.188414	0.646656
Validated nuclear estrogen receptor alpha network	21	0.191616	0.656206
Regulation of mitotic cell cycle	26	0.192377	0.656206
APC/C-mediated degradation of cell cycle proteins	26	0.192377	0.656206
mRNA Processing	48	0.193636	0.657699
Validated transcriptional targets of TAp63 isoforms	18	0.193813	0.657699
Mitotic Telophase /Cytokinesis	7	0.19518	0.657699
Polo-like kinase mediated events	7	0.19518	0.657699
eNOS activation and regulation	7	0.19518	0.657699

http://dx.doi.org/10.21037/jtd-20-3601

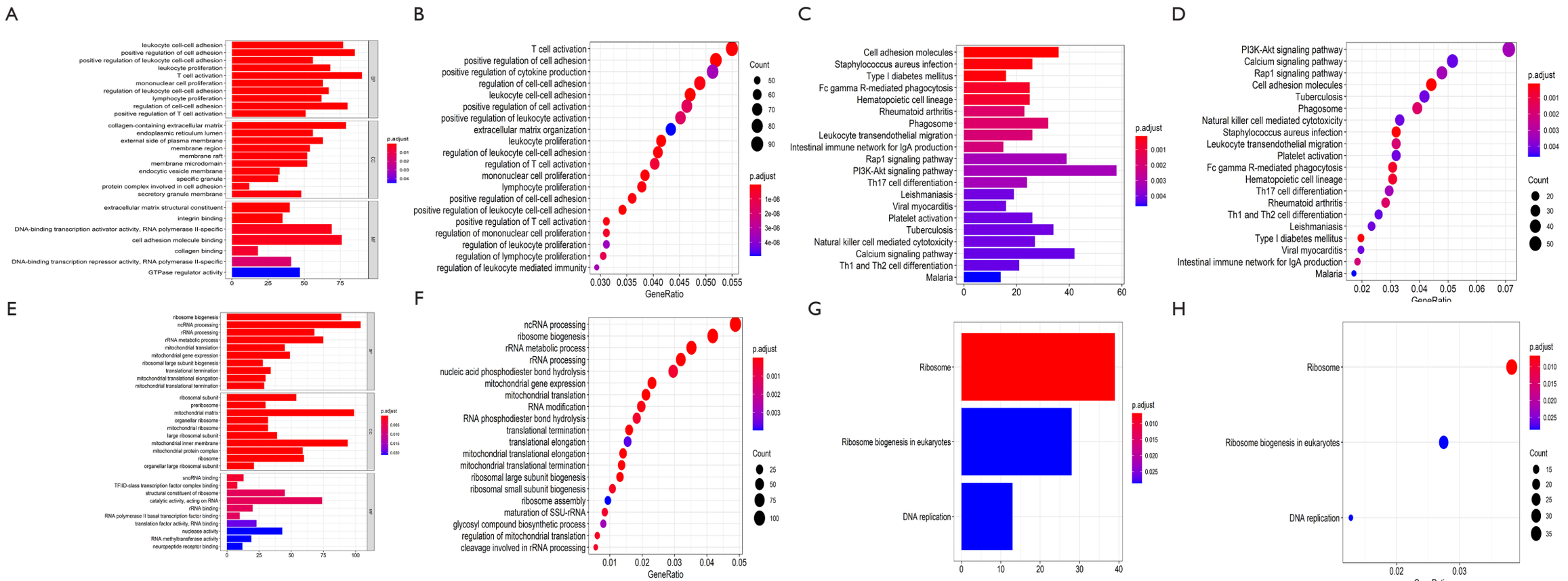

Figure S1 Functional enrichment analysis for DEGs. GO (A,B) and KEGG pathway (C,D) analysis for DEGs of GSE26155. GO (E,F) and KEGG pathway (G,H) analysis for DEGs of GSE9106. For bar plots, terms with top-10 significant adjusted P value were shown and were ordered according to adjusted P value. For dot plots, Terms with top-20 count number were ordered according to count number. For all these plots, redder color indicates smaller adjusted P value while bluer color indicates larger adjusted P value and all the adjusted P values of these terms were <0.05.

http://dx.doi.org/10.21037/jtd-20-3601

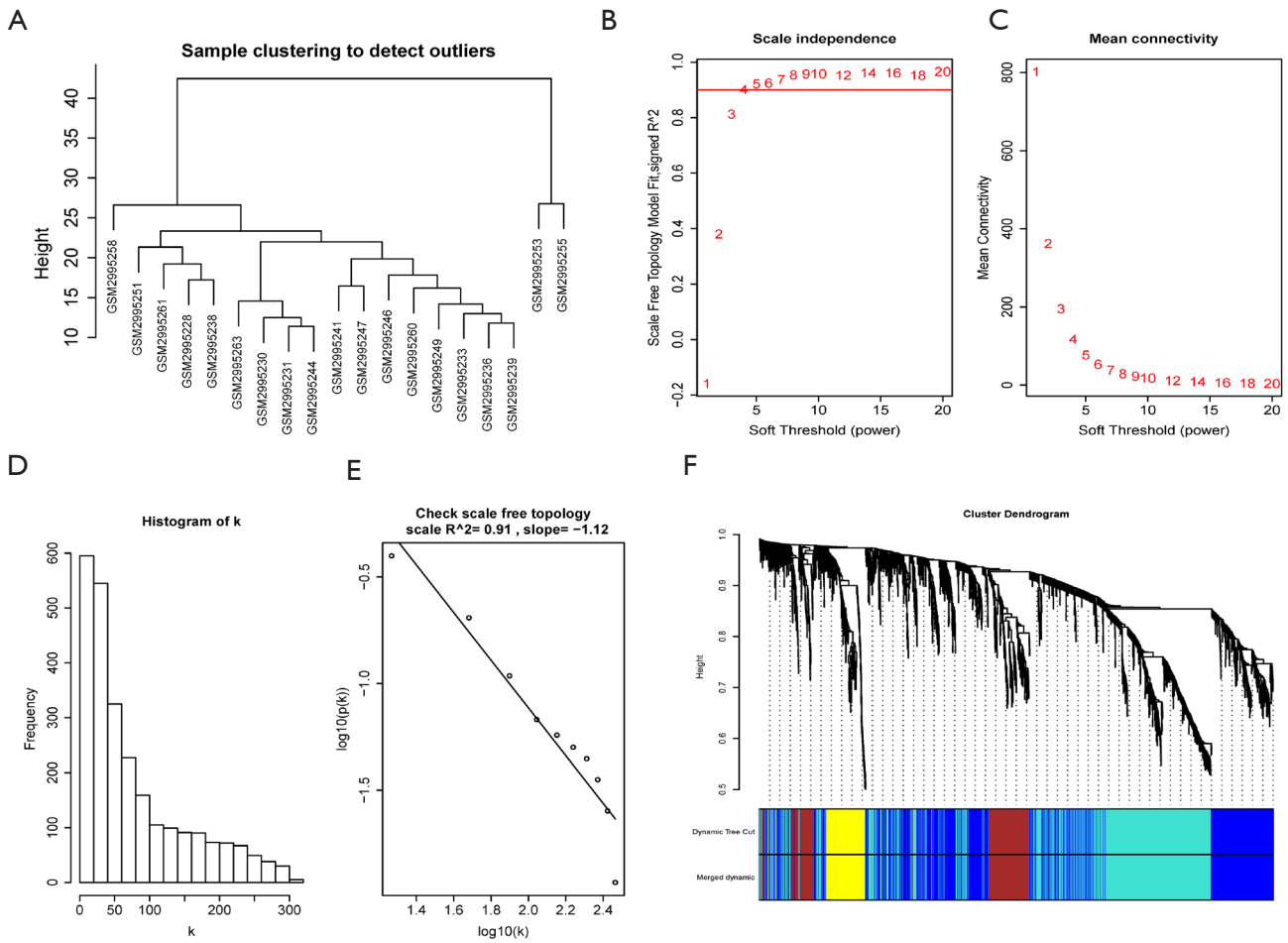

Figure S2 Construction of miRNA co-expression network for TAA. (A) No outlier was excluded in the analysis. (B,C) A soft threshold of β=5 was selected with a R2 cut-off of 0.9. (D,E) The constructed miRNA co-expression network met the requirement of scale-free topology. (F) Four miRNA modules were detected.

http://dx.doi.org/10.21037/jtd-20-3601

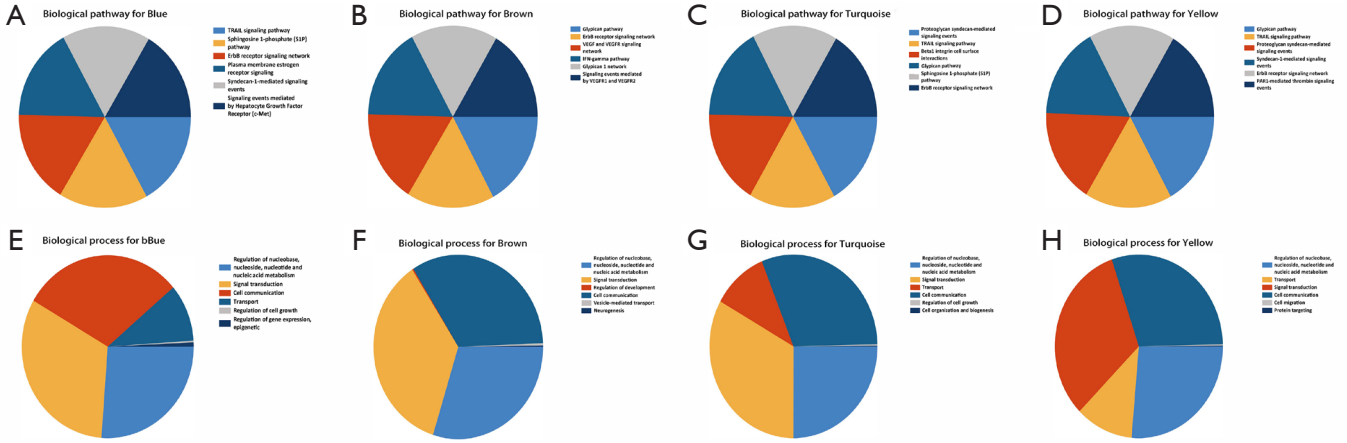

Figure S3 Functional enrichment analysis for miRNAs in different miRNA modules detected in the WGCNA analysis. (A,B,C,D) The biological pathways for the blue, brown, turquoise and yellow modules. Terms with top-6 significance are shown. (E,F,G,H) The biological processes for the blue, brown, turquoise and yellow modules. Terms with top-6 significance are shown.

http://dx.doi.org/10.21037/jtd-20-3601

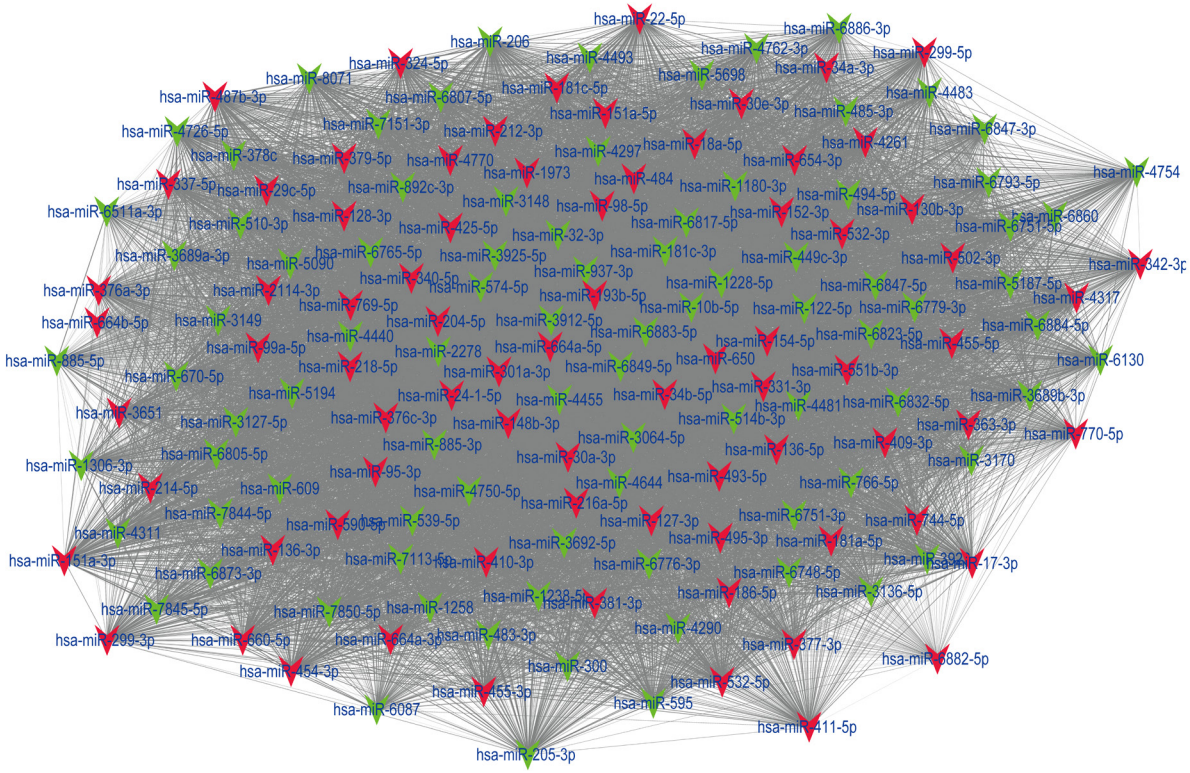

Figure S4 Interactions between crucial miRNAs and target genes predicted by the miRTarbase database.

http://dx.doi.org/10.21037/jtd-20-3601

Table S2 Functional enrichment of target genes predicted by miRTarbase

Terms	Count	adjusted P
GO		
protein stabilization	26	0.00178
intrinsic apoptotic signaling pathway in response to DNA damage by p53 class mediator	12	0.002192
regulation of protein stability	33	0.003663
regulation of apoptotic signaling pathway	41	0.00635
G1 DNA damage checkpoint	13	0.006533
intrinsic apoptotic signaling pathway	32	0.006533
DNA damage response, signal transduction by p53 class mediator resulting in cell cycle arrest	12	0.006533
signal transduction involved in mitotic G1 DNA damage checkpoint	12	0.006533
intracellular signal transduction involved in G1 DNA damage checkpoint	12	0.006533
intrinsic apoptotic signaling pathway by p53 class mediator	14	0.006533
embryonic organ development	41	0.006533
signal transduction involved in mitotic cell cycle checkpoint	12	0.006533
signal transduction involved in mitotic DNA damage checkpoint	12	0.006533
signal transduction involved in mitotic DNA integrity checkpoint	12	0.006533
morphogenesis of a branching epithelium	23	0.006533
negative regulation of response to DNA damage stimulus	14	0.007929
positive regulation of calcium-mediated signaling	10	0.007929
positive regulation of catabolic process	40	0.008028
protein homooligomerization	35	0.008028
intrinsic apoptotic signaling pathway in response to DNA damage	16	0.008028
nucleobase-containing compound transport	27	0.008028
mitotic G1 DNA damage checkpoint	12	0.008028
mitotic G1/S transition checkpoint	12	0.008028
regulation of intrinsic apoptotic signaling pathway	21	0.008315
RNA localization	26	0.008315
positive regulation of cellular catabolic process	35	0.011017
developmental growth involved in morphogenesis	26	0.011017
epithelial cell maturation	6	0.011017
morphogenesis of a branching structure	23	0.011017
cell growth	43	0.01138
signal transduction by p53 class mediator	28	0.01321
negative regulation of axonogenesis	12	0.014664
negative regulation of apoptotic signaling pathway	25	0.016657
viral gene expression	22	0.01758
positive regulation of mesenchymal cell proliferation	7	0.01758
positive regulation of cell cycle arrest	13	0.01758
regulation of developmental growth	33	0.01758
negative regulation of axon extension	9	0.01758
nucleic acid transport	22	0.01758
RNA transport	22	0.01758
developmental cell growth	25	0.017646
mammary gland development	18	0.018681
signal transduction involved in DNA integrity checkpoint	12	0.018681
signal transduction involved in DNA damage checkpoint	12	0.018681
establishment of RNA localization	22	0.01956
signal transduction involved in cell cycle checkpoint	12	0.020009
regulation of cell cycle arrest	15	0.020009
positive regulation of cyclin-dependent protein kinase activity	8	0.020628
regulation of cellular component size	34	0.020991
regulation of cell growth	37	0.021128
regulation of calcium-mediated signaling	14	0.021765
negative regulation of intrinsic apoptotic signaling pathway	14	0.021765
gland development	38	0.022541
proteasome-mediated ubiquitin-dependent protein catabolic process	37	0.022541
positive regulation of cell cycle	35	0.022711
cell cycle checkpoint	23	0.024683
regulation of protein complex disassembly	15	0.026528
negative regulation of developmental growth	15	0.026528
viral transcription	20	0.026528
embryonic skeletal system development	16	0.027225
interleukin-12-mediated signaling pathway	9	0.027225
anterior/posterior pattern specification	23	0.027225
mRNA transport	18	0.02759
negative regulation of growth	25	0.029546
proteasomal protein catabolic process	40	0.030875
cell aging	15	0.031475
neuron projection extension	19	0.03195
macroautophagy	28	0.03195
autophagy	41	0.03195
process utilizing autophagic mechanism	41	0.03195
thyroid gland development	6	0.03195
cellular response to interleukin-12	9	0.03195
embryonic skeletal system morphogenesis	13	0.03195
skeletal system morphogenesis	24	0.033093
negative regulation of neuron differentiation	23	0.033093
nose development	5	0.033189
cell cycle G1/S phase transition	28	0.033247
respiratory system development	21	0.033783
response to interleukin-12	9	0.033783
negative regulation of intrinsic apoptotic signaling pathway in response to DNA damage	7	0.033783
DNA damage checkpoint	17	0.034237
regulation of mRNA catabolic process	21	0.034237
ncRNA transcription	14	0.034237
negative regulation of cell growth	20	0.03512
gland morphogenesis	15	0.03512
regulation of proteolysis involved in cellular protein catabolic process	22	0.03512
axon extension	15	0.03721
negative regulation of neuron apoptotic process	17	0.03721
embryonic organ morphogenesis	27	0.03721
positive regulation of T cell activation	21	0.037819
regulation of cell cycle G1/S phase transition	21	0.037819
negative regulation of cell morphogenesis involved in differentiation	13	0.037819
mitotic DNA damage checkpoint	13	0.037819
regulation of ubiquitin-dependent protein catabolic process	17	0.04081
positive regulation of leukocyte cell-cell adhesion	22	0.04081
regulation of cellular protein catabolic process	24	0.040892
regulation of mesenchymal cell proliferation	7	0.041416
epithelial tube morphogenesis	29	0.041416
negative regulation of peptidyl-tyrosine phosphorylation	9	0.042403
G1/S transition of mitotic cell cycle	26	0.045173
mitotic cell cycle checkpoint	18	0.046059
regulation of protein tyrosine kinase activity	12	0.046059
regulation of response to interferon-gamma	6	0.046059
regulation of interferon-gamma-mediated signaling pathway	6	0.046059
regulation of calcineurin-NFAT signaling cascade	7	0.046059
regulation of calcineurin-mediated signaling	7	0.046059
negative regulation of neuron death	21	0.046968
regulation of signal transduction by p53 class mediator	19	0.046968
striated muscle tissue development	33	0.049507
response to hypoxia	31	0.049584
focal adhesion	42	0.000273
cell-substrate adherens junction	42	0.000273
cell-substrate junction	42	0.000273
ubiquitin ligase complex	29	0.007449
transferase complex, transferring phosphorus-containing groups	26	0.019143
transcription factor complex	33	0.019143
ubiquitin protein ligase binding	34	0.002369
ubiquitin-like protein ligase binding	35	0.002369
protein N-terminus binding	18	0.002369
cadherin binding	36	0.002614
protein kinase regulator activity	22	0.019133
protein kinase activator activity	13	0.023105
disordered domain specific binding	8	0.023105
cell adhesion molecule binding	44	0.024642
enhancer sequence-specific DNA binding	16	0.030572
kinase activator activity	13	0.031417
RNA polymerase II distal enhancer sequence-specific DNA binding	14	0.034729
KEGG_Pathway		
p53 signaling pathway	13	
Transcriptional misregulation in cancer	23	

http://dx.doi.org/10.21037/jtd-20-3601

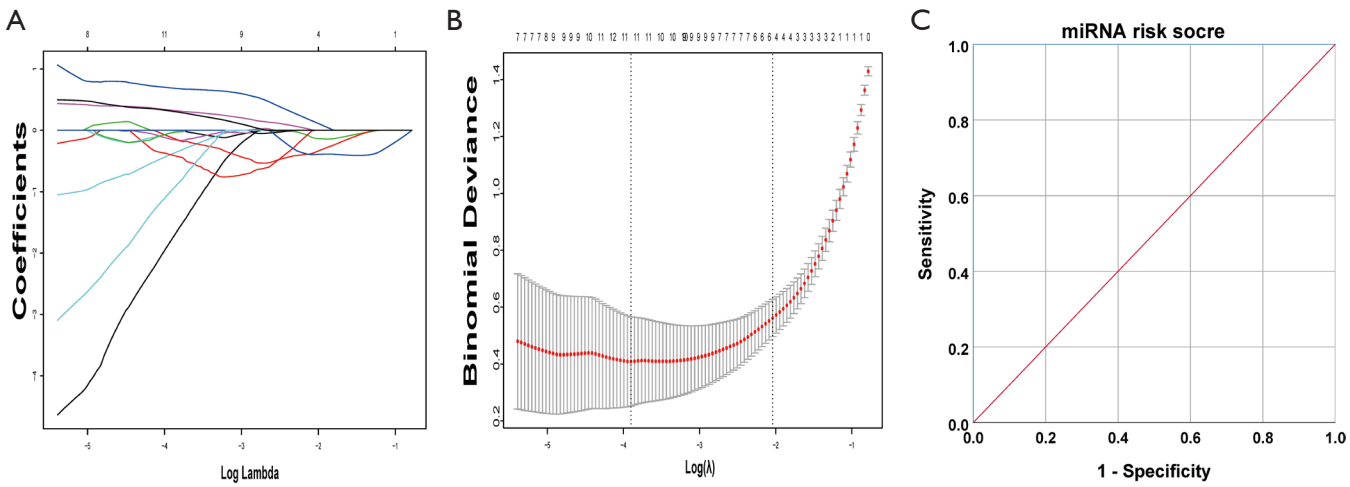

Figure S5 Calculation of miRNA risk score by LASSO regression. (A) LASSO coefficient profiles of 159 genes in MCODE cluster. (B) Ten-fold cross-validation for selecting minimal λ based on 1-SE criteria for recurrence. (C) A total of 11 miRNAs were selected to calculate a miRNA risk score.

http://dx.doi.org/10.21037/jtd-20-3601

Table S3 Coefficients for lasso regression

miRNA	Coef
hsa_miR_6882_5p	0.689211
hsa_miR_885_5p	-0.38507
hsa_miR_7845_5p	-1.76679
hsa_miR_7844_5p	-0.40415
hsa_miR_6849_5p	-0.03473
hsa_miR_6847_5p	-0.14738
hsa_miR_206	-0.12108
hsa_miR_6807_5p	-0.04007
hsa_miR_1306_3p	-0.9693
hsa_miR_128_3p	0.326034
hsa_miR_551b_3p	0.311317

http://dx.doi.org/10.21037/jtd-20-3601